

The University of Maine

DigitalCommons@UMaine

---

Electronic Theses and Dissertations

Fogler Library

---

Summer 8-20-2021

## Development of a Novel Haptic Feedback System for Gait Training Applications

Mohsen Alizadeh Noghani

University of Maine, mohsen.alizadeh@maine.edu

Follow this and additional works at: <https://digitalcommons.library.umaine.edu/etd>



Part of the [Biomechanical Engineering Commons](#), [Biomechanics Commons](#), [Biomechanics and Biotransport Commons](#), [Electro-Mechanical Systems Commons](#), [Motor Control Commons](#), and the [VLSI and Circuits, Embedded and Hardware Systems Commons](#)

---

### Recommended Citation

Alizadeh Noghani, Mohsen, "Development of a Novel Haptic Feedback System for Gait Training Applications" (2021). *Electronic Theses and Dissertations*. 3405.  
<https://digitalcommons.library.umaine.edu/etd/3405>

This Open-Access Thesis is brought to you for free and open access by DigitalCommons@UMaine. It has been accepted for inclusion in Electronic Theses and Dissertations by an authorized administrator of DigitalCommons@UMaine. For more information, please contact [um.library.technical.services@maine.edu](mailto:um.library.technical.services@maine.edu).

**DEVELOPMENT OF A NOVEL HAPTIC FEEDBACK SYSTEM FOR GAIT  
TRAINING APPLICATIONS**

By

Mohsen Alizadeh Noghani

B.Sc. Ferdowsi University of Mashhad, 2018

A THESIS

Submitted in Partial Fulfillment of the  
Requirements for the Degree of  
Master of Science  
(in Mechanical Engineering)

The Graduate School  
The University of Maine  
August 2021

Advisory Committee:

Babak Hejrati, Assistant Professor of Mechanical Engineering, Advisor

Mohsen Shahinpoor, Professor of Mechanical Engineering, Co-Advisor

Vincent Caccese, Professor of Mechanical Engineering

# DEVELOPMENT OF A NOVEL HAPTIC FEEDBACK SYSTEM FOR GAIT TRAINING APPLICATIONS

By Mohsen Alizadeh Noghani

Thesis Advisor: Dr. Babak Hejrati  
Thesis Co-Advisor: Dr. Mohsen Shahinpoor

An Abstract of the Thesis Presented  
in Partial Fulfillment of the Requirements for the  
Degree of Master of Science  
(in Mechanical Engineering)  
August 2021

Until recently, study and correction of motor or gait functions required costly sensors and measurement setups (e.g., optical motion capture systems) which were only available in laboratories or clinical environments. However, due to (1) the growing availability and affordability of inertial measurement units (IMUs) with high accuracy, and (2) progress in wireless, high bandwidth, and energy-efficient networking technologies such as Bluetooth Low Energy (BLE), it is now possible to measure and provide feedback in real-time for biomechanical parameters outside of those specialized settings. To enable gait training without an expert who can provide verbal feedback, augmented feedback, which is divided into three categories of visual, auditory, and haptic is necessary. Vibrotactile haptic feedback is of particular interest because it is both affordable and does not interfere with the situational awareness of the user. Among the systems proposed in the literature, there has been an absence of a system that is user-friendly, modular (i.e., it has individual, configurable sensing and feedback components), and completely wearable (i.e., all the components can be worn and carried by the user). In this work, we aim to address that gap by developing a novel wearable and modular smartphone-based system that provides vibrotactile feedback for gait training. The system's modularity and its smartphone-based controller and user interface can enhance its usability and promote regular gait training of

users, particularly older adults, during their daily living. Given the prevalence of stride length and speed decline in older adults, we developed a biomechanical data-driven approach to enable improving those outcomes via modifying their underlying surrogates. A subject study was performed by recruiting 12 young participants to assess the efficacy of the haptic system and our approach based on the notion of biomechanical surrogates. We found that the participants could significantly increase their thigh and shank extensions (i.e., the biomechanical surrogates) via the feedback provided by our system, and those increases led to higher values of stride length and walking speed. Our results provide a clear proof-of-concept for the developed biomechanics-driven haptic system for gait training of older adults to potentially improve their mobility and living independence.

## ACKNOWLEDGEMENTS

Parts of this thesis were previously published in Alizadeh Noghani et al. [1] © 2021 IEEE.

Mohsen Alizadeh Noghani, Mohsen Shahinpoor, and Babak Hejrati. “Design and Validation of a Smartphone-based Haptic Feedback System for Gait Training”. In: *IEEE Robotics and Automation Letters* 6.4 (2021), pp. 6593–6600.

## TABLE OF CONTENTS

|  |    |
|--|----|
| ACKNOWLEDGEMENTS .....   | ii |
| LIST OF TABLES .....   | v  |
| LIST OF FIGURES .....  | vi |
| 1. INTRODUCTION .....  | 1  |
| 1.1 Significance of Walking Speed in Older Adults .....                  | 2  |
| 1.2 Review of Tactile Feedback for Gait Training .....                   | 2  |
| 1.2.1 Knowledge of Result (KR) Strategy.....                             | 3  |
| 1.2.2 Knowledge of Performance (KP) Strategy .....                       | 6  |
| 1.3 Objectives of Thesis .....   | 10 |
| 2. IDENTIFICATION OF BIOMECHANICAL SURROGATES FOR STRIDE<br>LENGTH ..... | 12 |
| 3. HAPTIC FEEDBACK SYSTEM DESIGN .....                                   | 16 |
| 3.1 Hardware .....   | 16 |
| 3.2 Software .....   | 19 |
| 3.2.1 Feedback Algorithm .....   | 19 |
| 3.2.2 Measurement of the End-to-End Delay of the System .....            | 23 |

|   |    |
|---|----|
| 4. SUBJECT STUDY .....  | 26 |
| 4.1 Experiment Design .....   | 26 |
| 4.2 Results .....   | 28 |
| 4.2.1 Spatiotemporal Parameters .....                                 | 30 |
| 4.2.2 The Biomechanical Surrogates and TLA .....                      | 30 |
| 4.2.3 Symmetry Between the Two Sides in the TS Trial .....            | 31 |
| 4.2.4 Adjustment to Haptic Feedback .....                             | 32 |
| 4.2.5 Subjective Ratings by the Participants .....                    | 33 |
| 4.3 Discussion .....  | 33 |
| 4.3.1 Spatiotemporal Parameters .....                                 | 33 |
| 4.3.2 The Biomechanical Surrogates and TLA .....                      | 34 |
| 4.3.3 Symmetry Between the Two Sides in the TS Trial .....            | 35 |
| 4.3.4 Adjustment to Haptic Feedback .....                             | 35 |
| 4.3.5 Subjective Ratings by the Participants .....                    | 36 |
| 5. CONCLUSION .....   | 37 |
| APPENDIX A – SCHEMATIC OF THE MOTOR DRIVER PCB .....                  | 42 |
| APPENDIX B – LAYOUT OF THE MOTOR DRIVER PCB .....                     | 43 |
| APPENDIX C – THE PILOT PERCEPTION STUDY .....                         | 44 |
| APPENDIX D – INSTRUCTION SHEET SHOWN TO THE SUBJECTS .....            | 48 |
| APPENDIX E – PROCEDURE FOR OPERATING THE ANDROID<br>APPLICATION ..... | 49 |
| BIOGRAPHY OF THE AUTHOR .....   | 51 |

## LIST OF TABLES

|     |  |    |
|-----|--|----|
| 1.1 | Comparison of representative examples of tactile feedback systems used for gait training in the literature. .... | 11 |
| A.1 | The electronic parts used for the motor driver PCB. ....   | 42 |

## LIST OF FIGURES

|     |  |    |
|-----|--|----|
| 1.1 | Overview of the systems used to provide tactile feedback for training with KR strategy.....  | 4  |
| 1.2 | Examples of the systems used to provide tactile feedback for training with KP strategy.....  | 7  |
| 2.1 | Definition of the sagittal angles and segment frames.....  | 12 |
| 2.2 | The thigh, shank , and foot sagittal angles, the candidate surrogates, and heel strike and toe-off events for one gait cycle. .... | 14 |
| 2.3 | The data points and the fitted line showing the linear relationship between $T_{min}$ and normalized stride length. ....           | 15 |
| 3.1 | Schematic of the tactile haptic feedback system.....   | 17 |
| 3.2 | Size comparison of the components of the haptic feedback system and the system worn by a subject. ....                             | 19 |
| 3.3 | User interface of the developed Android application. ....  | 20 |
| 3.4 | Experiment setup for measuring the end-to-end delay. ....  | 24 |
| 3.5 | An example of measuring the delay using the IMUs' readings. ....   | 25 |
| 3.6 | Histogram of 100 delay measurements.....   | 25 |
| 4.1 | The walkway used for the subject study. ....   | 27 |
| 4.2 | Vectors and the angle used for calculating the trailing limb angle (TLA).....  | 29 |
| 4.3 | An example top-down view of a subject's right strides. ....  | 29 |

|     |   |    |
|-----|---|----|
| 4.4 | Bar graphs of cadence, normalized stride length, and normalized stride velocity for different trials. ....      | 30 |
| 4.5 | Bar graphs of The biomechanical surrogates and $TLA$ for different trials. ....                                 | 31 |
| 4.6 | Comparison of the surrogates and $TLA$ of the feedback and no-feedback sides in $TS$ condition. ....            | 32 |
| 4.7 | An example of plot $T_{min}$ and $S_{max}$ compared to their targets during feedback trials. ....               | 33 |
| C.1 | Schematic of the system designed for the pilot perception experiment. ....                                      | 44 |
| C.2 | A subject during the pilot perception experiment and the labeled keypad used for submitting the responses. .... | 46 |
| C.3 | Response accuracy at different locations and for different number of pulses. ....                               | 47 |

# CHAPTER 1

## INTRODUCTION

The ability to live independently requires maintaining a healthy gait and walking speed and is an essential aspect of aging successfully. It has been reported that 35% of community-dwelling adults over 70 years old suffer from neurological and/or nonneurological gait abnormalities, and those with abnormal gait experience more adverse health outcomes [2]. Recent findings suggest that the central nervous system and mobility are closely linked, and gait abnormalities are risk factors for cognitive decline, mild cognitive impairment, and dementia [3, 4, 5]. Due to association of walking speed with a variety of clinical outcomes such as hospitalization and mortality, it has been identified as the sixth vital sign [6]. Therefore, gait training or rehabilitation of older adults in early stages of aging to reduce future complications due to declining walking speed should be considered.

Measurement of the patient's performance and providing feedback accordingly is at the core of gait training and rehabilitation. For providing feedback, several methods such as verbal (by a human expert), visual, and haptic (tactile and kinesthetic) exist. Because tactile stimuli does not interfere with the vision and hearing of the patient and thus their situational awareness, it is particularly suitable for gait training and has been widely used in the systems developed in the literature [7]. Despite those significant advances, the systems proposed in the literature have had several shortcomings limited their usability in real-world environments.

In the next sections of this chapter, the previous research regarding tactile feedback systems for gait training is reviewed and their limitations are discussed. Additionally, the biomechanical motivation for increasing stride length and walking speed as the training outcome is detailed. Finally, the objectives and contributions of this work are presented.

## 1.1 Significance of Walking Speed in Older Adults

Walking speed has important associations with a variety of health outcomes in older adults. Mielke et al. [4] found a relationship between faster gait speed and better cognitive performance. In an eight-year longitudinal study of well-functioning (at the initial session) older adults with more than 2300 participants, about 25% of the subjects saw a rapid decrease in their walking speed, which was found to be a risk factor for mortality [8]. In contrast, Hardy et al. [9] found that improvements in normal walking speed during a one-year period was associated with a significantly reduced risk of mortality, even after taking multiple factors such as psychological and medical conditions into account. Another longitudinal study of community-dwelling adults found a link between slow walking speed and an elevated risk of mortality due to cardiovascular causes [10]. Further, slower walking speeds have been associated with an increased fall risk, even after adjustment for cognitive and physical decline [11]. Therefore, monitoring walking speed and rehabilitation for improving it has been recommended as a potential course of action for enhancing the health of older adults [8, 10].

The question that arises next is what could be the mechanism for improving the walking speed of that population. In terms of the high-level spatiotemporal gait parameters, the decrease in walking speed can, in theory, be a result of declines in stride length and/or cadence. Samson et al. [12] found that the reduction of walking speed was not associated with a drop in cadence, but rather with a decline in stride length. Similar results have been found in multiple other studies [13, 14, 15, 16, 17]. Thus, gait training to increase stride length could be a viable method for improving walking speed.

## 1.2 Review of Tactile Feedback for Gait Training

In gait training and motor learning applications, it is essential to provide timely feedback to the patient during the execution of the task. Traditionally, the feedback has been provided in the form of instructions by a therapist. However, augmented feedback,

which can be divided into three broad categories of visual, auditory, and haptic has shown promise for motor learning tasks [18]. Haptic feedback, which is categorized into two groups of kinesthetic (i.e., force feedback) and tactile, does not directly interfere with the visual or auditory sensing of the user; therefore, compared to the two other modalities, it is particularly suitable for gait training applications, especially outside of a controlled laboratory or clinical environment as avoiding impairment of the situational awareness of the user is key. Kinesthetic haptic feedback for rehabilitation can be particularly beneficial for individuals who need high levels of assistance such as spinal-cord-injury and post-stroke patients [19]. However, with the population of older adults who can walk independently yet demonstrate age-related deficits in their gait (e.g., decreased speed and stride length), using kinesthetic feedback devices may not be a suitable option. It has been suggested that age-related gait deficits such as reduced speed and stride length mainly stem from impaired neural control of movement which is revealed by poor coordination and timing, rather than low force production by muscles [20]. Therefore, providing tactile feedback, specifically in the form of vibrotactile stimuli, has become a common strategy in wearable devices used for gait training research [7].

In terms of gait training strategy, feedback can be given according to either knowledge of result (KR) or knowledge of performance (KP) [18]. In KR, feedback is provided by comparing the the user’s performance against a high-level objective. In contrast, in KP, the feedback signals that surrogate variables, on which the high-level objective depends on, should be adjusted. We next provide a review of the previous works that used tactile feedback with either strategy for gait training. The studies that used KR are discussed first and KP follows.

### **1.2.1 Knowledge of Result (KR) Strategy**

An overview of the systems used in the studies which adopted KR strategy is shown in Fig. 1.1.

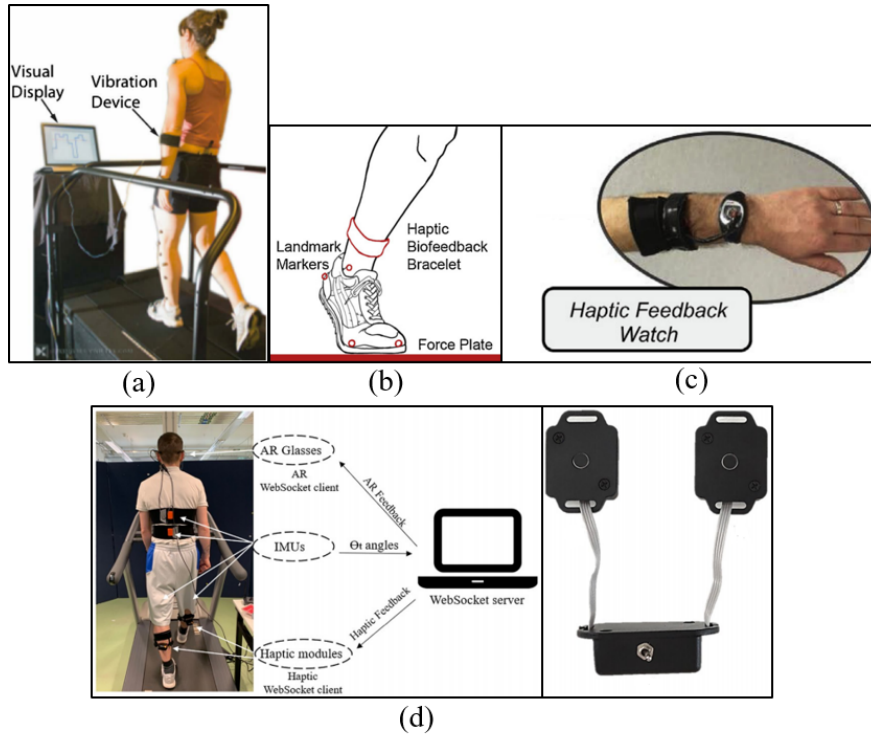


Figure 1.1: Overview of the systems used to provide tactile feedback for training with KR strategy. (a) Wheeler et al. [21], (b) Schneck et al. [22], (c) Sheerin et al. [23], and (d) Braga et al. [24].

Wheeler et al. [21] (Fig. 1.1a) compared the performance of visual and vibrotactile feedback, the latter applied on the forearm, in reducing the first peak of knee adduction moment (KAM). Reducing KAM can result in alleviating the pain and slowing the progression of medial compartment knee osteoarthritis (knee OA). Data from an instrumented treadmill and an optical motion capture systems were used to estimate KAM in a MATLAB program. In the haptic modality, the amplitude of vibration was based on the achieved decreased of KAM, and could be set to three levels with lower amplitudes corresponding to better performance, and no feedback when KAM was decreased the parameters by more than 40%. In the visual feedback trial, a screen installed in front of the subject displayed the baseline value and the subject's performance for the current and the previous 9 cycles. Instructions before the trials included general strategies that the subjects could try such as "loading inside or outside of the foot" and "changing the

distance between the feet". While both modalities achieved a reduction of about 20% on average, the subjects were able to adapt more quickly with the visual feedback. This can be attributed the advantage of using a display in showing the history of the subject's performance, and thus providing more information in the visual mode.

Schenck et al. [22] (Fig. 1.1b) provided tactile feedback on the shank to adjust the participants' peak ankle moment which is low in clinical populations such as post-stroke patients. Ankle moment was estimated by a LabVIEW program on a PC using data from an optical motion capture system and an instrumented treadmill. To indicate success, a "haptic bracelet" on the dominant shank, which connected to the LabVIEW program via Bluetooth was used to apply vibrotactile feedback when the estimated moment reached or exceeded the target. The subjects were divided into two groups; one received minimal verbal instructions and the other which received more detailed instructions that were repeated during the trials. Each group completed one trial (Feedback High) where the objective was to increase the moment compared to baseline, and another (Feedback Low) where the goal was to decrease it. In Feedback High, the change in the peak moment was not statistically significant, but peak ankle power increased. In Feedback Low, a significant decline in both the peak moment and power was reported. The difference between the two verbal instructions methods was not significant.

KR strategy was also used by Sheerin et al. [23] (Fig. 1.1c) for training to reduce the tibial acceleration, which is a surrogate for the risk of fracture of tibia due to fatigue in frequent runners. Acceleration data was measured with an IMU (inertial measurement unit) on the shank and sent to a PC, where it was processed using a LabVIEW program. A "haptic feedback watch", worn on the wrist, provided vibrotactile feedback when acceleration exceeded a threshold. To avoid receiving feedback, the participants were instructed to soften their footfalls. The subjects participated in 8 sessions with feedback which consisted of treadmill running for up to 30 minutes in the final session. The portion of the trial during which the subjects received feedback was gradually lowered from 100%

during the first session to only 10% in the final one. To investigate whether training on a treadmill translated to overground running, pre-intervention, post-intervention, and 4-weeks post-intervention results of running on a track were compared. Comparison of treadmill (overground) running to pre-intervention showed a decrease of 50% (28%) in the last session and 41% (17%) in the assessment four weeks after that.

Braga et al. [24] (Fig. 1.1d) compared two feedback modalities of visual, provided via augmented reality (AR) glasses, and tactile, applied through vibration motors, in terms of performance in adjusting knee misalignment angle and subject preference. The system was made up of an IMU-based motion capture system, a PC, an AR glass, and haptic modules consisting of a ESP8266 microcontroller, a vibration motor, and a battery. A PC received the data from the motion capture system, calculated the knee misalignment angle, and communicated with the haptic module or the AR glass (through WebSocket protocol) in case feedback was necessary. No tactile feedback was provided when the subject was able to reach the desired angle, whereas the visual feedback was always displayed. Overall, the young adult participants were more successful in adjusting their gait with visual feedback through the AR glasses than the vibrotactile mode.

### **1.2.2 Knowledge of Performance (KP) Strategy**

Desirable outcomes in walking can be abstract and difficult to convey to the user and it can be preferable to achieve the outcome through adjusting specific parameters; therefore, in KP strategy, relationships obtained from statistical analysis of biomechanical data are used to define the high-level outcomes in terms of adjusting surrogate variables. Some of the systems that used this strategy are presented in Fig. 1.2.

Dowling et al. [25] (Fig. 1.2a) investigated the efficacy of verbal and haptic feedback for reducing peak KAM. The surrogate for peak KAM was lateral load on the foot; in the verbal feedback trial, the instruction given to the participants was to minimize the weight on the lateral side of their foot. In addition to confirmation from the subject, their gait was

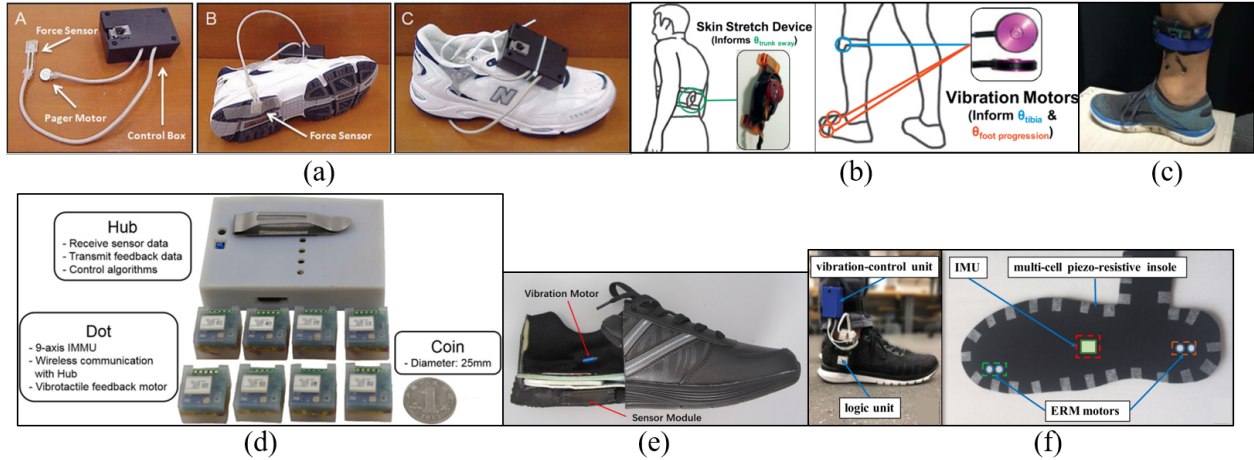


Figure 1.2: Examples of the systems used to provide tactile feedback for training with KP strategy. (a) Dowling et al. [25], (b) Shull et al. [26], (c) Chen et al. [27], (d) Xu et al. [28], (e) Xia et al. [29], and (f) Zhang et al. [30].

visually monitored during the trial to verify their compliance. A haptic feedback system consisting of force sensor, a shaftless eccentric mass vibration motor, and control electronics, was attached to the right shoe during the feedback trials. The force sensor was placed under the lateral side of the shoe and the vibration motor was placed inside the lateral side of the shoe. When the value read from the force sensor exceeded a threshold, the motor vibrated and provided feedback to user to adjust their gait. A reduction of 14.3% was achieved for the peak KAM in the haptic feedback trial, compared to only 8.3% with verbal feedback.

Foot progression angle (FPA), tibia angle, and trunk sway were used as the surrogates in a study by Shull et al. [26] (Fig. 1.2b). Vibrotactile cues were produced on the foot for FPA and on the shank for the tibia angle, and skin stretch in a circular pattern on the lower back informed trunk sway. A MATLAB program used data from an optical motion capture system and an instrumented treadmill to calculate the surrogates in real-time and provide feedback when the subject was not successful in reaching the target. For each subject, a single-parameter trial (i.e., feedback provided for one parameter at a time) was conducted first to explore the relationship between the surrogates and KAM. Using the results, the target values for each parameter were set for use in a data-driven training trial

with the goal of increasing peak KAM by at least 20%. In that trial, feedback was provided for all three surrogates simultaneously. Of the 9 young adults participants, eight were able to achieve a 30% decrease (range: 29-48%) of KAM. In a related study of knee OA patients [31], a decrease in FPA, resulting in a toe-in gait, was targeted as the surrogate for peak KAM by applying feedback to the shank. On average, the subjects were able to achieve a  $5^\circ$  decrease in FPA which translated to a 13% reduction of peak KAM.

KP strategy was also employed in a six-week gait training study of knee OA patients by Shull et al. [32]. Baseline, weekly training sessions over 6 weeks, post-training and one-month post-training assessments were compared for both subjective pain ratings of the subjects, the FPA, and the peak KAM. Additionally, during the 6 weeks, the subjects were instructed to practice the modified gait for at least 10 minutes per day at home and had to fill activity logs. In the 1-month followup, subjective pain ratings were significantly lower than the baseline; additionally, an average 16% decrease in peak KAM was maintained during the 1 month follow-up assessment, which can be compared to 9% for other non-invasive means such as using specialized shoe soles and 33% as a result of surgery.

Xu et al. [28] (Fig. 1.2d) designed a wireless and modular tactile feedback system with configurable units ("Dots") that could be used for either sensing or feedback. Each Dot consisted of a vibration motor, an IMU, a microcontroller, and a battery embedded in silicon, and communicated with a central unit ("Hub") via Zigbee protocol. The Hub received data from the sensing Dots at 50 Hz, processed and stored it on a micro-SD card, executed the feedback algorithm, and transmitted messages to the feedback Dots in case feedback was necessary. The performance of the system was assessed in a preliminary study where feedback was provided for FPA as a surrogate for KAM. A sensing Dot on the dorsal side of the foot was used for measuring FPA, and two feedback Dots on the lateral and medial aspects of the shank provided feedback when the FPA was outside of the no-feedback zone in toe-in or toe-out gait training.

Xia et al. [29] (Fig. 1.2e) embedded the sensing, processing, and feedback components required for providing feedback for FPA in a shoe to create a self-contained feedback system. An electronics module, consisting of a microcontroller, which recorded the data on a SD card, an IMU, and a battery, was placed in the shoe sole. Two vibration motors in the shoe and on the lateral and medial sides provided vibrotactile feedback when FPA moved outside of a no-feedback window. The performance of the system was validated with a preliminary study on young adult subjects.

Step width (SW) and FPA were used as the surrogates for KAM by Chen et al. [27] (Fig. 1.2c). A LabVIEW program calculated the two surrogates using data from an optical motion capture system and an instrumented treadmill. Two distinct feedback schemes, binary pulses and tactile apparent motion, were used for each parameter and all subjects tried both scenarios (i.e., tactile apparent motion for SW and binary pulses for FPA, and vice-versa) with a washout period of at least two days between the trials. Success was defined as reaching the objectives for 80% of a block of 20 right steps, and inability to achieve that in 500 steps was deemed a failure. The majority of the young adults subjects (9 out of 10) were able to attain the targets set for the surrogates, but no interaction was found between the number of steps required for training and the feedback scheme.

Zhang et al. [30] (Fig. 1.2f) aimed to change walking speed through adjusting walking cadence (i.e., the surrogate) using a concept similar to rhythmic auditory simulation (RAS). In RAS, the patient (e.g. stroke or Parkinson's) is instructed to walk in concert with an audio stimulus (e.g. a metronome or a music track) with a specific tempo; this can improve coordination, and by selecting a high-tempo track, walking speed. Similarly, the system designed by Zhang et al. provided vibrotactile stimulus to the foot, and the subjects had to adjust their gait such that the initial contact of the foot coincided with the haptic feedback. The sensing and feedback components of the system used to identify the gait events, calculate the spatiotemporal parameters, and provide feedback (the piezo-resistive force sensors, an IMU, and vibration motors) were embedded in the shoe insole and

connected to an electronics unit attached to the outside of the shoe and on the lateral side which communicated with a single-board computer (e.g. a Raspberry Pi) through Wi-Fi. For feedback strategy, two methods were investigated. In the open loop method, feedback was applied at pre-determined intervals, whereas in the closed loop, the timing of feedback varied with the subject's error with respect to the target speed. The young adult subjects performed three types of overground walking trials in terms of the target cadence and each trial was done with both the open loop and closed loop method. Overall, it was found that (1) the feedback did not significantly affect the variability of neither walking speed nor cadence, and (2) the subjects performed better in following the speed trajectory with the closed loop method, and the cadence trajectory with the open loop strategy.

### 1.3 Objectives of Thesis

Four features are critical for the usability of a haptic feedback system in community- and home-based settings. It is crucial for a system to be (1) wearable, where the entire system could be worn and carried by users [28, 29, 30], (2) wireless, where the sensors and feedback modules are not connected to the main control unit by wires [23, 28, 24] (3) modular, where there are separate feedback and sensing units that can be placed on different body parts and replaced as needed [23, 28, 24], and to have (4) a user-friendly interface/controller for intuitive interactions. In Table 1.3, seven representative systems from the literature are compared based on those criteria. Currently, there is an absence of a system that has all the four features simultaneously, and the development of such a system was the first objective of this work (Chapter 3).

Motivated by the importance of walking speed and its decline due to decreasing stride length in older adults, the second objective was establishing a correlation between stride length and lower-extremity surrogates that would be appropriate for applying feedback (Chapter 2). Finally, the third goal was verifying that relationship by gait training of human subjects using the haptic feedback system (Chapter 4).

| Target population   | Target parameter                           | Feedback location            | Sensors            | Controller  | Modular | Wireless | Wearable |
|---------------------|--|------------------------------|--------------------|---|---------|----------|----------|
| Zhang et al. [30]   | Older adults                               | Cadence                      | Foot               | Piezo-resistive force sensor, IMU                     | $\mu$ C | ×        | ✓        |
| Xia et al. [29]     | Osteoarthritis patients                    | FPA                          | Foot               | IMU   | $\mu$ C | ✓        | ✓        |
| Xu et al. [28]      | N/A  | N/A                          | N/A                | IMU   | $\mu$ C | ✓        | ✓        |
| Shull et al. [27]   | Osteoarthritis patients                    | FPA, trunk sway, tibia angle | Foot, shank, trunk | Optical motion capture system, instrumented treadmill | PC      | ×        | ×        |
| Chen et al. [27]    | Osteoarthritis patients                    | FPA, step width              | Shank              | Optical motion capture system, instrumented treadmill | PC      | ×        | ×        |
| Sheerin et al. [23] | Runners                                    | Tibial acceleration          | Wrist              | IMU   | PC      | ✓        | ×        |
| Braga et al. [24]   | People with knee varus/valgus misalignment | Knee valgus/varus            | Shank              | IMU   | PC      | ✓        | ×        |

Table 1.1: Comparison of representative examples of tactile feedback systems used for gait training in the literature.

## CHAPTER 2

### IDENTIFICATION OF BIOMECHANICAL SURROGATES FOR STRIDE LENGTH

Our goal was to use statistical analysis to identify lower extremity segment (the thigh, shank, and foot) angles that (1) had a significant correlation with stride length, (2) could be readily measured in real-time, and (3) were appropriate for applying feedback in terms of ability of users to modify them as well as placement of measurement and feedback components.

We considered the angles of the three lower-limb segments in the sagittal plane, shown by  $\theta_T$ ,  $\theta_S$ , and  $\theta_F$  in Fig. 2.1. Gait data of 14 young adult subjects (8 males, 6 females,  $23.8 \pm 3.3$  years,  $1.74 \pm 0.92$  m) were used from a previous study [33], in which the subjects were asked to walk on a treadmill at self-selected normal and fast speeds while their full-body kinematics were recorded using a Vicon motion capture system (Vicon Motion Systems, Oxford, UK). Data processing to obtain the segment angles and stride length was carried out in Visual3D (C-Motion, Rockville, Maryland, USA). Each segment was assumed to be a rigid body in 3D space, and we defined the sagittal segment angles as the angle of rotation around the  $X$ -axis in a  $ZYX$  Euler rotation sequence describing the orientation of the segment frames (Fig. 2.1) relative to their initial orientation (i.e., with the subject in a neutral posture).

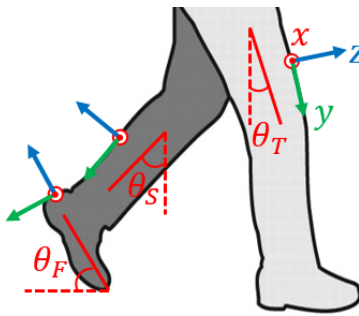


Figure 2.1: Definition of the sagittal angles and segment frames.

Often, segment frames are tracked using both a marker cluster on the segment and anatomical landmarks where locating the latter depends on the judgment of the person placing the markers and is therefore prone to uncertainty and error. In order to minimize that problem, the frames were defined using only the marker clusters for the thighs and shanks, and the clusters as well as heel and toe markers for the feet. Heel strikes were defined as the maxima of the location of the heel markers in the direction of walking with respect to the the pelvis segment. Stride length was obtained by adding the distance between the locations of the heel marker in consecutive heel strikes to the distance travelled by the treadmill belt during that interval.

The following five parameters within a gait cycle, as shown in Fig. 2.2, were considered as the candidates for the surrogates and, thereby, for training: the maximum and minimum thigh angle ( $T_{max}$ ,  $T_{min}$ ), the maximum and minimum shank angle ( $S_{max}$ ,  $S_{min}$ ), and the maximum foot angle ( $F_{max}$ ). Note that  $T_{max}$  and  $S_{max}$  correspond to the thigh flexion and shank extension, respectively, and  $F_{max}$  occurs close to heel strike. Also,  $T_{min}$  and  $S_{min}$  correspond to the thigh extension and shank flexion, respectively. These five parameters were selected because (1) we hypothesized their modifications could be conveyed to the subjects via haptic feedback, and (2) they were straightforward to calculate in real-time by a peak finding method.

In each trial and for each subject, the sagittal angles and height-normalized stride length were obtained for 20 strides for each leg. The normalized value was used to account for the variability of the subjects' height and thus make the results more generalizable. To determine the biomechanical surrogates for training, we used multiple linear regression in SPSS v26 (IBM Corporation, Armonk, NY, USA) with height-normalized stride length ( $\bar{L}$ ) as the dependent variable and the mentioned five parameters as the independent variables. We focused on finding two surrogates since, in terms of the perception of the haptic stimuli, it would be impractical to provide feedback for more than two parameters during a single gait cycle.  $T_{min}$  (i.e., the thigh extension) was found to be the best predictor of

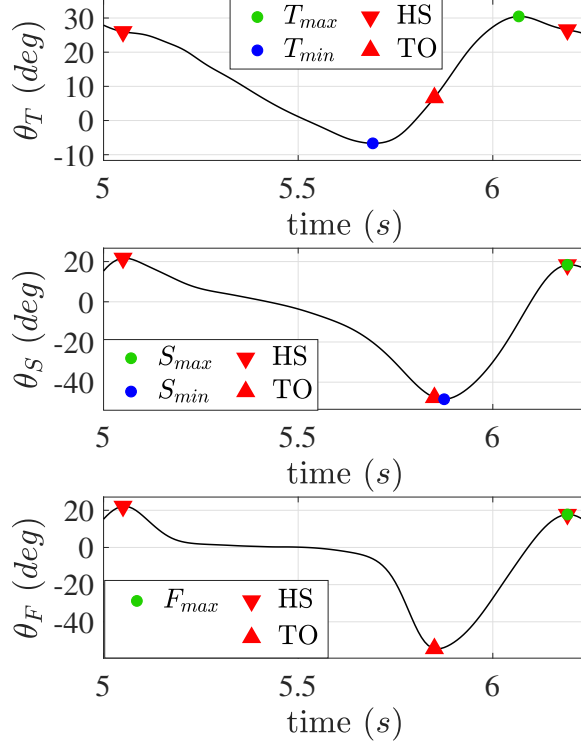


Figure 2.2: The thigh (top), shank (middle), and foot (bottom) sagittal angles, the candidate surrogates, and heel strike (HS) and toe-off (TO) events shown for one gait cycle.

stride length ( $R^2 = 0.782$ ), and, therefore, it was selected as the first surrogate. The linear relationship between  $T_{min}$  and  $\bar{L}$  is illustrated in Fig 2.3.

In choosing the second surrogate, a major consideration was to maximize the perceptibility of the haptic stimuli. Cholewiak et al. [34] tested discrimination of two vibrotactile patterns for two durations of stimuli (4 ms and 52 ms) and for multiple values of interstimulus interval (ISI) on the fingers and palm of the hand, and on the thigh. It was found that the accuracy of identifying the pattern increases with higher values of ISI. Other studies have found that the ability to distinguish between vibrotactile feedback decreases when they are provided at multiple locations at the same time [35, 36]. In another work, Plaisier et al. [37] observed that the participants were able to better distinguish vibrotactile stimuli on the back as the distance between them increased. In summary, the perceptibility of tactile stimuli is higher the more the stimuli are separated

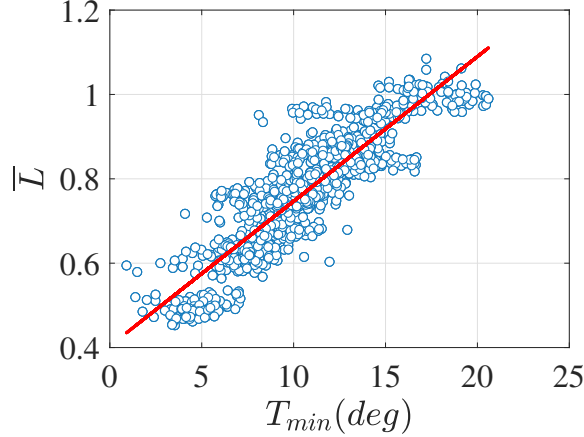


Figure 2.3: The data points and the fitted line showing the linear relationship between  $T_{min}$  and normalized stride length ( $R^2 = 0.782$ ).

temporally and spatially. Therefore, we focused on a parameter spatially distant from thigh and temporally delayed from occurrence of  $T_{min}$ .

Those considerations excluded  $T_{max}$  (the same segment as  $T_{min}$ ) and  $S_{min}$  (occurring at roughly at the same time as  $T_{min}$ ) from the potential candidates. The remaining parameters in the statistical model were  $F_{max}$  ( $\Delta R^2 = 0.093, p < 0.001$ ) and  $S_{max}$  ( $\Delta R^2 = 0.036, p < 0.001$ ). We chose  $S_{max}$  (i.e., the shank extension) as the second surrogate due to an easier and more reliable placement of haptic feedback components on the shank and because we hypothesized that an increase in  $F_{max}$  could be achieved as a result of increasing  $S_{max}$ . The final model used  $T_{min}$  and  $S_{max}$  with  $R^2 = 0.818$ , indicating these two variables could explain more than 80% of variability in stride length during walking.

Thus,  $T_{min}$  and  $S_{max}$  were considered as the biomechanical surrogates for stride length and their positive correlations in the statistical model suggested that increasing one or both could be a mechanism for increasing stride length. To determine the target values for  $T_{min}$  and  $S_{max}$  for training with the haptic feedback system, we compared the increases in the average values of  $T_{min}$  and  $S_{max}$  during fast walking relative to normal walking both in terms of percentage ( $T_{min} : 54\%$ ,  $S_{max} : 17\%$ ) and absolute difference ( $\Delta \bar{T}_{min} : 4.5^\circ$ ,  $\Delta \bar{S}_{max} : 3.7^\circ$ ).

## CHAPTER 3

### HAPTIC FEEDBACK SYSTEM DESIGN

A schematic of the haptic feedback system is shown in Fig. 3.1. The user's thigh and shank angles were measured by IMUs which sent the orientation data in real-time through Bluetooth Low Energy (BLE) to the control system implemented on a smartphone. In the control algorithm,  $T_{min}$  and  $S_{max}$  were extracted for each cycle and compared to the target; if they were smaller than the target, requests for feedback were sent to the microcontroller in the electronics units to activate the vibrotactors for informing the user to modify their gait.

#### 3.1 Hardware

We chose an Android smartphone, Pixel 3a (Google, Mountain View, CA, USA), as the main processing unit. The most important feature and advantage of a smartphone compared to a single-board computer such as a Raspberry Pi is that, in addition to a fast processor, it includes a screen (which is essential for providing a graphical user interface), a durable battery, and a Wi-Fi router in a small and lightweight device. There is no other combination of hardware components that could provide those in comparably small and well-integrated package. Therefore, we believe that using a smartphone to provide an intuitive interface for user interactions and as the main controller and data logger of the system can promote usability and acceptability of the system, and reduce stigma related to using a training device among older adults. Additionally, by comparing a smartphone to other options in the initial phases of this research, we found that it provides the most reliable hardware and software stack for BLE, the protocol commonly used by wearable IMUs.

Six Xsens DOT IMUs (Xsens Technologies B.V., Enschede, The Netherlands), each with 25 g of mass and with a dynamic orientation error of  $1^\circ$  RMS ( $1\sigma$ ), were placed one on

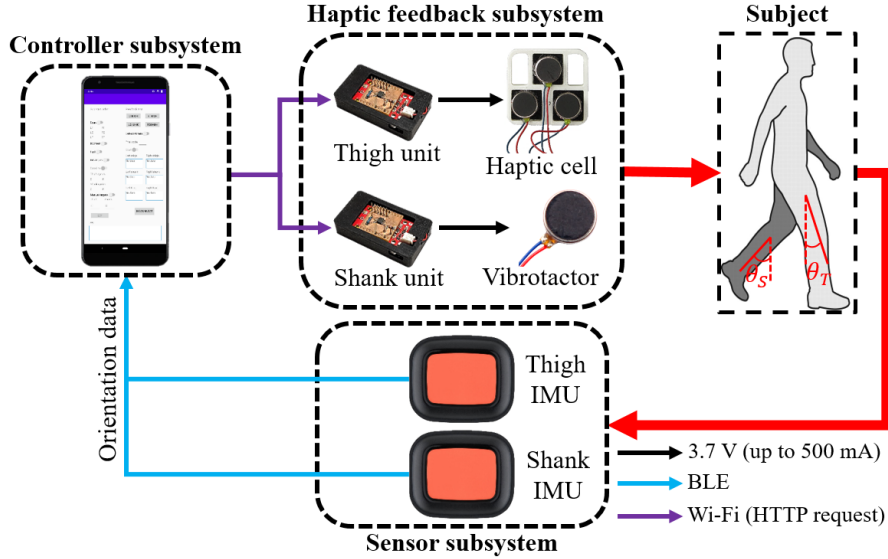


Figure 3.1: Schematic of the tactile haptic feedback system.

each thigh, shank, and foot, sending orientation in quaternion form and free acceleration components in the earth-fixed frame at 60 Hz to the phone via BLE 5.0. Four electronics units (85 g,  $68 \times 38 \times 14$  mm) were used in total, and they were attached to the lateral side of the thighs and shanks (one on each segment) using double-sided tapes. Each unit consisted of an ESP8266 Thing microcontroller (SparkFun, Boulder, CO, USA), a custom circuit board for driving the vibrotactor(s) (Appendices A and B), and an 850 mAh battery all enclosed in a 3D-printed case. By using the custom PCB, up to 500 mA at the battery voltage could be provided to the motors whereas the Input/Output pins supplied only up to 12 mA, which would not be sufficient for operation of the motors at their rated current. Overall, the system’s architecture provided the flexibility necessary for using different numbers of sensing and feedback components and placing them at different locations on the body.

To provide vibrotactile feedback, inexpensive and generic shaftless vibration motors, referred to as vibrotactors from hereon, were utilized. For the thigh, we designed a “haptic cell” (25 g,  $37 \times 34 \times 6$  mm) consisting of three vibrotactors (12 mm diameter, 3.6 mm height, 75 mA at 3.7 V, purchased from Amazon) in a parallel circuit and attached them to

a 3D-printed base in an equilateral triangle configuration (Fig. 3.1). The pairwise distance between the vibrotactors was 16 mm, well below the two-point distance threshold for the thigh (7 cm)[38], and they were connected to the base by a hook and loop fastener allowing them to vibrate about their resting positions. Using 3 vibrotactors as described created a larger stimulation area for increasing the likelihood of perceiving the feedback and minimized the bending of wires, while ensuring that adequate current for the cells' operation was supplied. The haptic cells were placed on the posterior side of each thigh to cue increasing the thigh extension (and thus  $T_{min}$ ). For applying feedback to each shank to cue increasing the shank extension (and therefore  $S_{max}$ ), we attached a single vibrotactor (10 mm diameter, 3.6 mm height, 75 mA at 3.7 V, purchased from Pololu) to its anterior side. The haptic cells and the vibrotactors were connected to the custom circuit board of the electronics unit, which supplied up to 500 mA at 3.7 V to the vibrotactor(s). Fig. 3.2a illustrates the size of the components of the system, and Fig. 3.2b shows the system worn by a subject.

The haptic cells and the vibrotactors were connected to the custom circuit board of the electronics unit, which supplied up to 500 mA at 3.7 V to the vibrotactor(s). Acceleration measurements were analyzed to identify the characteristics of the vibrotactors such as the dominant frequency and peak-to-peak acceleration. Acceleration was measured at 800 Hz with a BNO055 IMU attached to the vibrotactor. 15 individual 0.5 second vibrations were analyzed and the results were averaged. By performing spectral analysis, the dominant frequency was found to be close to 240 Hz, which is about the frequency corresponding to the maximum sensitivity of the Pacinian mechanoreceptors of human skin (245 Hz) [39]. For both types of vibrotactors, our estimate of the maximum peak-to-peak acceleration for a system with a total mass of 100 g is  $55 \frac{m}{s^2}$ . The total added mass was 135 g for each thigh and 120 g for each shank. We estimate the battery life of the system in continuous use (i.e., with the IMUs streaming data at 60 Hz) to be about 3 hours, limited by the battery life of Xsens DOT sensors.



Figure 3.2: (a) Size comparison of the components of the haptic feedback system. (b) The system worn by a subject.

We should note that perceptibility of feedback through the haptic cells was validated in a preliminary perception experiment with 4 healthy older adults which is discussed in Appendix C.

## 3.2 Software

### 3.2.1 Feedback Algorithm

When turned on, each ESP8266 microcontroller searched for a Wi-Fi network created by the phone and established a connection to the network. Then, it started an HTTP server, meaning that after receiving data in the form of HTTP requests via Wi-Fi, it would interpret the message and take an appropriate action such as turning the vibrotactor(s) on. We developed an Android application with the following four essential functionalities: (1) receiving data from the four IMUs on the thighs and shanks through BLE, (2) processing and (3) logging the data, and (4) sending HTTP requests to the microcontrollers for providing haptic feedback, in which case the vibrotactors were turned on for 0.5 seconds. The user interface of the application is shown in Fig. 3.3 and the typical procedure for operating it is discussed in Appendix E.

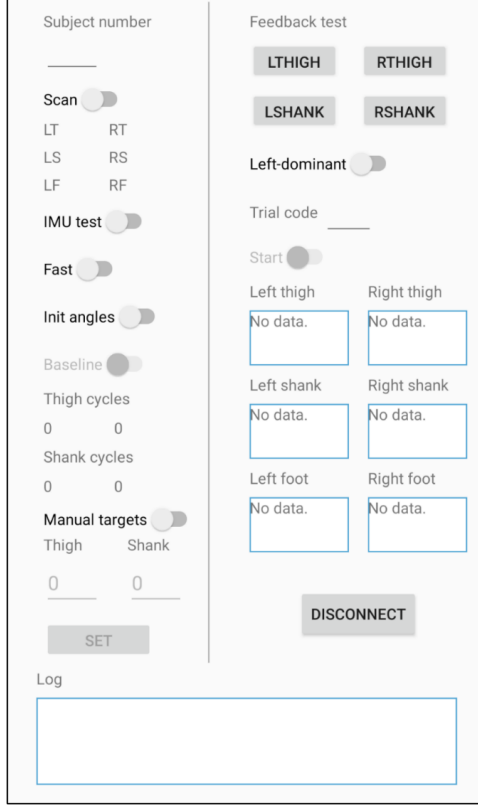


Figure 3.3: User interface of the developed Android application.

A simplified pseudocode for the core functions of haptic feedback system is presented in Algorithm 1 which will be discussed next.

Each IMU was placed on the subject such that the sensor frame  $S$  was oriented similarly to the segment frames shown in Fig. 2.1. The IMUs sent the absolute orientation of the sensor frames with respect to a local earth-fixed frame  $E$  in the form of a unit quaternion  ${}^S\mathbf{q}_E$ ,

$${}^S\mathbf{q}_E = (q_0, q_1, q_2, q_3) \quad (3.1)$$

Frame  $E$  was defined using the ENU convention, meaning that  $\hat{\mathbf{x}}_E$  axis pointed to the east,  $\hat{\mathbf{y}}_E$  to the north, and, importantly, the  $\hat{\mathbf{z}}_E$  to the "up" direction (i.e., opposite the gravity vector). The sagittal angle was defined as the change in the angle between  $\hat{\mathbf{z}}_E$  and  $\hat{\mathbf{z}}_S$  which we denote by  $\theta$ . From the definition of the rotation matrix  ${}^S\mathbf{R}_E$ , its elements can

---

**Algorithm 1** Pseudocode of the haptic feedback algorithm
 

---

**Parameters:**

$d_{peaks}$  ▷ Minimum number of samples between peaks  
 $threshold$  ▷ Minimum value of a peak

**Input:** Data packet containing  ${}^S\mathbf{q}_E = (q_0, q_1, q_2, q_3)$ 

```

1:  $C_{packet} \leftarrow C_{packet} + 1$  ▷ Packet counter
2:  $\theta \leftarrow \arccos(1 - 2q_1^2 - 2q_2^2)$ 
3:  $\theta_k \leftarrow \theta - \theta_0$ 
4: if  $C_{packet} \geq C_{peak} + d_{peaks}$  and  $\theta_{k-1} > threshold$  and  $\theta_{k-1} > \theta_k$  and  $\theta_{k-1} > \theta_{k-2}$  then
5:    $C_{peak} \leftarrow C_{packet}$  ▷  $\theta_{k-1}$  is a peak
6:   if  $\theta_{k-1} - target < 0$  then ▷ Give feedback
7:      $C_{success} \leftarrow 0$  ▷ Reset the success counter
8:     Send HTTP request for giving feedback.
9:   else ▷ No feedback
10:     $C_{success} \leftarrow C_{success} + 1$ 
11:    if  $C_{success} == 5$  then ▷ Increase the target
12:       $C_{success} \leftarrow 0$ 
13:       $target \leftarrow target + \delta_{target}$ 
14:  $\theta_{k-2} \leftarrow \theta_{k-1}$ 
15:  $\theta_{k-1} \leftarrow \theta_k$ 
16: Update the CSV log with the packet's data.

```

---

be written in terms of the dot products of the unit vectors of the two frames' axes [40].

$${}^S\mathbf{R}_E = \begin{bmatrix} \hat{\mathbf{x}}_E \cdot \hat{\mathbf{x}}_S & \hat{\mathbf{x}}_E \cdot \hat{\mathbf{y}}_S & \hat{\mathbf{x}}_E \cdot \hat{\mathbf{z}}_S \\ \hat{\mathbf{y}}_E \cdot \hat{\mathbf{x}}_S & \hat{\mathbf{y}}_E \cdot \hat{\mathbf{y}}_S & \hat{\mathbf{y}}_E \cdot \hat{\mathbf{z}}_S \\ \hat{\mathbf{z}}_E \cdot \hat{\mathbf{x}}_S & \hat{\mathbf{z}}_E \cdot \hat{\mathbf{y}}_S & \hat{\mathbf{z}}_E \cdot \hat{\mathbf{z}}_S \end{bmatrix} \quad (3.2)$$

The direction vectors in eq. 3.2.1 have a magnitude of 1. In turn, the matrix elements simplify to the cosine of the angles between the vectors, commonly known as the direction cosine matrix (DCM). Therefore, the angle can be obtained from the third diagonal element of the rotation matrix.

$$\theta = \arccos(\hat{\mathbf{z}}_E \cdot \hat{\mathbf{z}}_S) = \arccos(R_{33}) \quad (3.3)$$

Because the orientation is provided in quaternion form, the third diagonal element of the rotation matrix can be expressed using that parameterization as follows [40],

$$R_{33} = 1 - q_1^2 - q_2^2 \quad (3.4)$$

Therefore, the angle between  $\hat{\mathbf{z}}_E$  and  $\hat{\mathbf{z}}_S$  can be calculated using the equation below,

$$\theta = \arccos(1 - q_1^2 - q_2^2) \quad (3.5)$$

To calculate the sagittal angle, it is necessary to obtain the initial angle of the two axes ( $\theta_0$ ) first. To that end, in each trial, the subjects were asked to stand still before starting to walk and the quaternion measurements were collected for three seconds (180 samples). The quaternion representation of the initial orientation ( ${}^I\mathbf{q}_E$ ) was calculated by averaging the 180 samples and converting the result ( $\bar{\mathbf{q}}_0$ ) to a unit quaternion as shown in eq. (3.6) and eq. (3.7).

$$\bar{\mathbf{q}}_0 = \frac{\sum_{i=1}^{180} {}^S\mathbf{q}_E}{180} \quad (3.6)$$

$${}^I\mathbf{q}_E = \frac{\bar{\mathbf{q}}_0}{\|\bar{\mathbf{q}}_0\|} \quad (3.7)$$

Then, the initial sagittal angle  $\theta_0$  was obtained using (3.3) and was subtracted from the angle measured during walking at time  $k$  to obtain the sagittal angle denoted by  $\theta_k$  in Algorithm 1. A peak finding algorithm was employed to detect  $T_{min}$  and  $S_{max}$ . As shown in Algorithm 1, it used two tunable parameters of  $d_{peaks}$  (minimum number of samples between peaks) and  $threshold$  (minimum value of a peak). In the version of the algorithm used for this study,  $d_{peaks}$  was set to 30 for both the thighs ( $T_{min}$ ) and shanks ( $S_{max}$ ) and  $threshold$  was set to 4 and 10 degrees for the thighs ( $T_{min}$ ) and shanks ( $S_{max}$ ), respectively. After finding the peak, it was compared to its corresponding target value. If the peak was smaller than the target value, an asynchronous HTTP request was sent from the Android program to the electronics unit, activating the haptic cell or vibrotactor for 0.5 second. The vibration duration of 0.5 second was chosen based on its high perceptibility in a pilot study with older adults (as discussed in Section 3.1) as well as its successful use in other gait training research [41, 31, 29]. If the subject was able to maintain the target value for 5 consecutive cycles, the target value was increased by half of either  $\Delta\bar{T}_{min}$  or  $\Delta\bar{S}_{max}$ , and this increase is denoted by  $\delta_{target}$  in Algorithm 1. Given the placement of the haptic cells

on the posterior side of the thighs (to increase  $T_{min}$ ) and the vibrotactors on the anterior side of the shanks (to increase  $S_{max}$ ), the haptic feedback scheme utilized a “pull towards target” metaphor found to be superior to the “push away from target” metaphor in terms of subject preference [41].

### 3.2.2 Measurement of the End-to-End Delay of the System

It was important to characterize the delay of the system in providing feedback as the subject should have adequate time for responding to it before the next gait cycle. The following are the 5 primary sources of delay from the occurrence of a peak angle (whether  $T_{min}$  or  $S_{max}$ ) in the physical world to the vibration of the corresponding vibrotactor(s) on the skin: (1) data processing in the IMU, (2) sending data from the IMU to the smartphone through BLE, (3) processing in the Android application (including the peak detection algorithm), (4) sending data from the phone to the ESP8266 microcontroller through WiFi, and (5) processing the HTTP message in the microcontroller. Although the rise time of the vibrotactor could also be calculated by fitting an envelope on the measured acceleration signal [37], that is not directly dependent on the architecture of the system and therefore will not be discussed.

Ultimately, we are interested in the total delay (i.e., the total time from when when the IMU measures a peak smaller than the target to the start of vibration of the motor on the corresponding segment) because this is an important factor for providing feedback in a timely manner. We used the following experiment, with the setup shown in Fig. 3.4, to measure the delay. Similar to an actual gait training experiment, all the IMUs and the electronics units were connected to the smartphone. The right shank IMU and another IMU (which we call Segment IMU) were placed inside the displayed enclosure to ensure that they have the same orientation. In the Android application, the feedback for the right shank was enabled, and the target angle was set to 75 degrees. Another IMU (Motor IMU) was attached with double-sided tape to the right shank’s vibrotactor to measure the

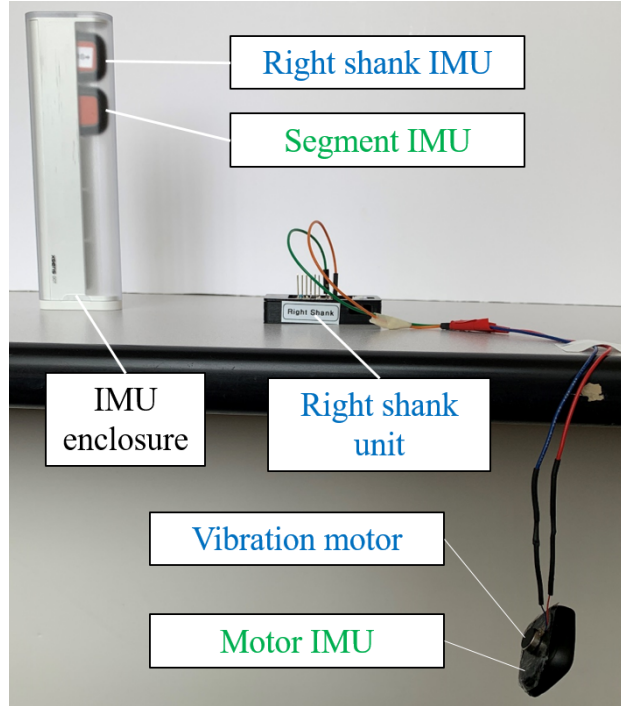


Figure 3.4: Experiment setup for measuring the delay. The components with blue labels are connected to the Android application. The IMUs with green labels are connected to another phone and measure data at 120 Hz with synchronized timestamps.

acceleration signal in case of feedback and thus vibration. The start of vibration was defined as the first large change in the acceleration magnitude (with the offset removed) and was found by inspection. An example of total delay calculation is illustrated in Fig. 3.5.

In order to trigger feedback, the enclosure was manually rotated to an angle smaller than 75 degrees and back. By repeating the procedure for 100 times, the delay was estimated to be  $137 \pm 53$  milliseconds. This value is comparable to the delay of 120 ms reported by Xu et al. [28] (the standard deviation and the number of measurements were not provided) for adjusting gait parameters using their wireless system, which was deemed sufficiently short. Also, the delay is small when considering the 1-second period of a typical human gait cycle as reported in the literature [12]. Additionally, the histogram for the 100 measurements is presented in Fig. 3.6, which shows that 91% of the measurements had a delay below or equal to 200 ms.

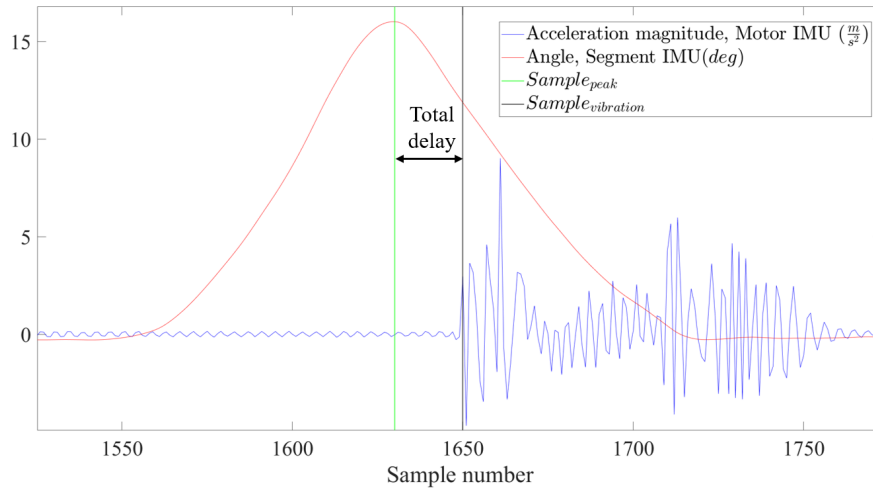


Figure 3.5: An example of measuring the delay using the IMUs' readings. For clarity, the offset of the acceleration magnitude (about 9.81) is removed.

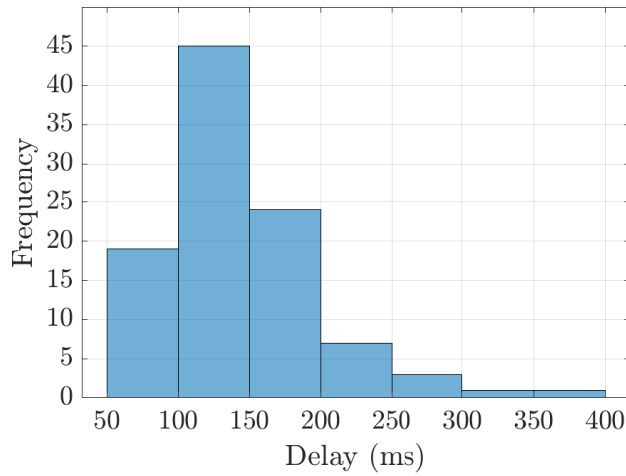


Figure 3.6: Histogram of 100 delay measurements.

## CHAPTER 4

### SUBJECT STUDY

To verify the choice of the surrogates and to validate the functionality of the developed haptic feedback system, a subject study was conducted. The primary goal was to demonstrate if and how increasing  $T_{min}$  and  $S_{max}$  would translate into higher values of stride length. Further, the effect of changing the surrogates on other gait parameters were investigated and subjective ratings about the system and feedback were collected.

#### 4.1 Experiment Design

The experiments were conducted on a 54 m  $\times$  3 m U-shaped walkway shown in Fig. 4.1. First, the feedback system was placed on the subject. Then, 7 trials were performed in the following order (notations in parentheses are used throughout this paper to refer to the experimental conditions),

- Trial 1 ( $F$ ): the subject was asked to walk at their self-selected fast speed.
- Trial 2 ( $N$ ): the subject was asked to walk at their self-selected normal speed. During this trial, starting from the sixth detected peak and using the next 20 peaks, the averages of the surrogates,  $\bar{T}_{min}$  and  $\bar{S}_{max}$ , were calculated to establish their baseline values. Using the percentage increases reported in Chapter 2, initial targets were set at  $1.54\bar{T}_{min}$  and  $1.17\bar{S}_{max}$ .
- Trial 3 (familiarization trial): we explained the experimental procedure to the subject. For familiarization, feedback was provided for either the thigh or shank of the dominant side, and the subject was asked to modify their gait upon receiving feedback.
- Trial 4 (both thighs:  $TT$ , both shanks:  $SS$ ): feedback was given on both the left and right sides of the target segment of Trial 3.



Figure 4.1: The walkway used for the subject study.

- Trials 5-6: Similar to 3-4, but for the other segment.
- Trial 7 (*TS*): feedback was given for the shank and thigh of the dominant side, and the subject was asked to replicate their adjustments on the other side as well to maintain a symmetric movement.

The instruction sheet which was used to inform the subjects about how to react to the feedback is presented in Appendix D. During each trial, the subjects walked for one lap on the walkway. A two minute break was provided between the trials. Regarding the order of the trials, Trials 1, 2, and 7 were fixed, and the single-segment trials (Trials 3 and 5) always preceded the double-segment trials of the corresponding segment (Trials 4 and 6). The number of subjects who tried the feedback on their thighs first and then their shanks was equal to the number of those who tried the reverse order. After completing the experiment, the subjects filled out a questionnaire evaluating the haptic feedback on the

thigh and shank by rating the following on a scale of 0-10 for each segment: (a) level of comfort (a higher score meant more comfort), (b) noticeability (a higher score meant more noticeable), and (c) intuitiveness for reaching the target (a higher score meant more intuitive). Finally, the length of thigh and shank segments were defined as the distance between skeletal landmarks and measured using a tape,

- Thigh length: From the greater trochanter to the lateral side of the knee joint.
- Shank length: From the lateral side of the knee joint to the lateral side of the ankle joint.

## 4.2 Results

Twelve healthy adults (8 males, 4 females, 19-39 years range with an average of  $25.5 \pm 5.8$  years,  $1.72 \pm 0.11$  m,  $74.3 \pm 15.6$  kg), were recruited to participate in the experiment, which was approved by University of Maine’s IRB. The subjects were healthy, with no history of musculoskeletal or gait problems and did not have any prior experience with the haptic system. Data processing was carried out in MATLAB (MathWorks, Natick, MA, USA) to obtain the spatiotemporal parameters of interest (cadence, height-normalized stride length  $\bar{L}$ , and height-normalized stride velocity  $\bar{V}$ ) and changes in the surrogates ( $T_{min}$  and  $S_{max}$ ). Also, given the importance of the trailing limb angle (TLA) in generating propulsive forces during walking [42], it was calculated using  $\theta_T$  and  $\theta_S$ . TLA was defined as the maximum of the angle between the vertical axis and the vector sum of the thigh and shank vectors, with the positive direction indicated in Fig. 4.2. To compute stride length from the foot orientation and acceleration data, we utilized the method presented by Sabatini et al. [43]. Acceleration of the foot segment in the local earth-fixed frame, measured by the IMU attached to the shoe, was integrated to obtain the linear velocity. In order to remove the drift due to bias and noise in the signal, a zero-velocity update method was utilized, where the velocity was assumed to be zero at the midstance. An example output is shown Fig. 4.3.

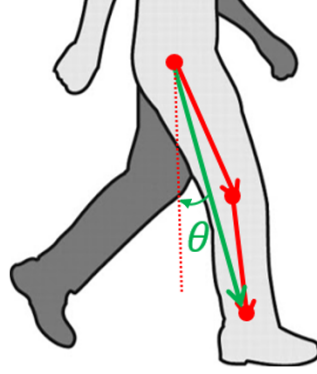


Figure 4.2: Vectors and the angle used for calculating the trailing limb angle (TLA).

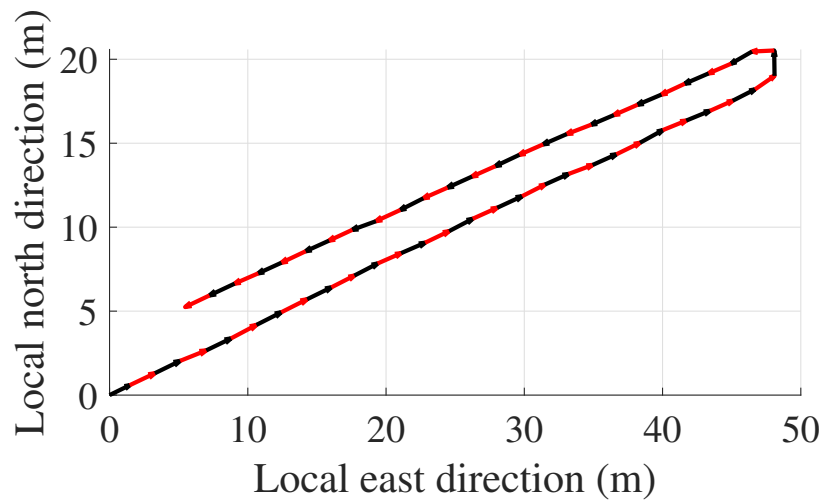


Figure 4.3: An example top-down view of a subject's right strides. Each stride vector starts at a heel strike and ends at the next. The colors alternate for clarity.

In each trial, the mentioned parameters during 30 cycles of steady-state walking for each leg were obtained and averaged. Statistical analysis was performed in SPSS and significance level was set at  $\alpha = 0.05$ . One-way repeated measures ANOVA was used to test for statistically significant differences among the five conditions. Mauchly's test was used to check the sphericity assumption, and if it was rejected, Greenhouse-Geisser correction was applied. Post-hoc analysis with Bonferroni correction was performed to find the pairs with a significant difference.

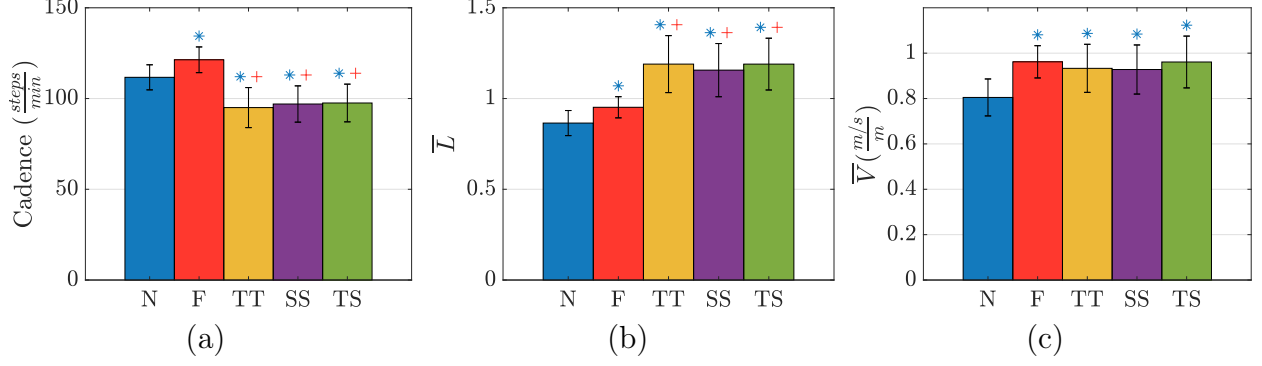


Figure 4.4: (a) Cadence, (b) normalized stride length, and (c) normalized stride velocity for different conditions. Error bars represent  $\pm 1$  standard deviation. Asterisks and plus signs denote statistically significant differences ( $p < 0.05$ ) in pairwise comparisons with respect to  $N$  and  $F$  conditions, respectively.

#### 4.2.1 Spatiotemporal Parameters

Fig. 4.4 shows the bar charts of cadence, normalized stride length, and normalized stride velocity for normal walking, fast walking, and the three feedback conditions. There were statistically significant differences for all the three parameters as follows: cadence ( $F(2.33, 25.6) = 28.7, p < 0.001$ ),  $\bar{L}$  ( $F(1.6, 17.6) = 52.2, p < 0.001$ ),  $\bar{V}$  ( $F(2.42, 26.6) = 8.79, p = 0.001$ ). Post-hoc analysis revealed that there was a significant difference in cadence between  $N$  and  $F$  conditions and between all the feedback conditions with both  $N$  and  $F$ ; however, no significant difference was found among  $TT, SS, TS$ . Similar results were found for  $\bar{L}$ . While there were significant differences in  $\bar{V}$  between  $N$  and all the other conditions, no difference was found between  $F$  and the feedback conditions. Compared to  $N$  condition,  $\bar{L}$  increased by 10% in  $F$ , 37.6% in  $TT$ , 33.7% in  $SS$ , and 37.6% in  $TS$ . Also compared to  $N$  condition,  $\bar{V}$  increased by 19.5% in  $F$ , 15.9% in  $TT$ , 15.3% in  $SS$ , and 19.4% in  $TS$ .

#### 4.2.2 The Biomechanical Surrogates and TLA

The bar plots for the surrogates and TLA in different conditions are shown in Fig. 4.5. Significant differences were found across the conditions:  $T_{min}$  ( $F(1.84, 20.2) = 55.3, p < 0.001$ ),  $S_{max}$  ( $F(4, 44) = 62.6, p < 0.001$ ), and  $TLA$

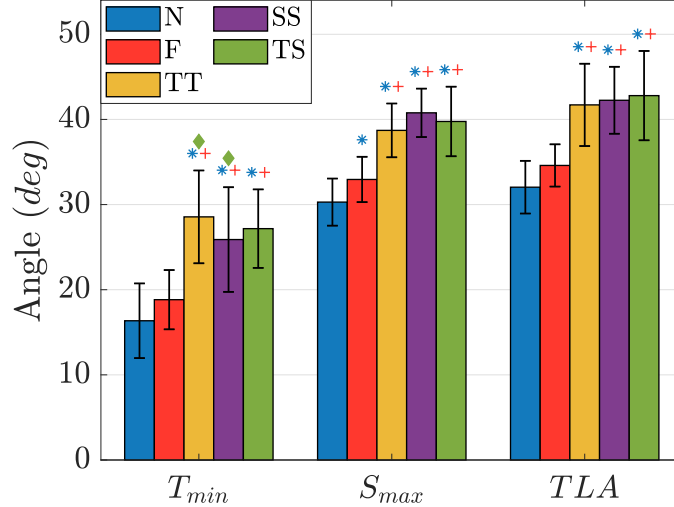


Figure 4.5: The biomechanical surrogates and  $TLA$  for different conditions. Asterisks and plus signs denote statistically significant differences in pairwise comparisons to  $N$ ,  $F$  conditions, respectively. Diamonds (only shown for the feedback conditions) show significant difference in comparison to  $TS$ .

( $F(4, 44) = 56.2, p < 0.001$ ). Post-hoc analysis for  $T_{min}$  found a significant difference for all the pairs except for  $N - F$  ( $p = 0.111$ ),  $TT - TS$  ( $p = 0.069$ ), and  $SS - TS$  ( $p = 0.884$ ). Post-hoc analysis for  $S_{max}$  revealed a significant difference for all the pairs except between feedback trials ( $p > 0.178$ ). The pairwise comparison results for  $TLA$  were similar to  $S_{max}$ , with the exception of no significant difference between  $N - F$  ( $p = 0.194$ ). Compared to normal walking,  $T_{min}$  increased by 74.6% in  $TT$ , 58.3% in  $SS$ , and 66.2% in  $TS$ ;  $S_{max}$  increased by 27.8% in  $TT$ , 34.6% in  $SS$ , and 31.3% in  $TS$ . In addition, significant differences were identified among the conditions for  $F_{max}$  ( $F(1.47, 16.2) = 39.8, p < 0.001$ ). While post-hoc analysis no significant differences among the feedback conditions, they were significantly different from  $N$  and  $S$ . Compared to normal walking,  $F_{max}$  increased by 21.5% in  $TT$ , 20.9% in  $SS$ , and 22.3% in  $TS$ .

### 4.2.3 Symmetry Between the Two Sides in the TS Trial

We compared the spatiotemporal parameters and biomechanical surrogates between the feedback and no-feedback sides in  $TS$  condition (i.e., feedback only on the dominant thigh and shank) using paired t-tests. All the variables passed the Shapiro-Wilk test of

normality. The differences between spatiotemporal parameters were not statically significant ( $p = 0.96$  for cadence,  $p = 0.71$  for  $\bar{L}$ , and  $p = 0.88$  for  $\bar{V}$ ). As for the surrogates (Fig. 4.6), there were significant differences for both  $T_{min}$  ( $t(11) = 2.73, p = 0.020, 3.3^\circ$  higher mean for the feedback side) and  $S_{max}$  ( $t(11) = 2.42, p = 0.034, 2.1^\circ$  higher mean for the feedback side), but not for  $TLA$  ( $t(11) = 0.039, p = 0.0969$ ). In other feedback conditions of  $TT$  and  $SS$ , where the feedback was applied to both sides, no significant differences were found between the two sides for neither the surrogates,  $T_{min}$  ( $p > 0.127$ ),  $S_{max}$  ( $p > 0.069$ ), nor  $TLA$  ( $p > 0.120$ ).

#### 4.2.4 Adjustment to Haptic Feedback

We investigated the subjects' ability to increase the biomechanical surrogates upon receiving feedback on the corresponding segment. Starting from initial target values for the surrogates, the target angles were gradually increased when the subjects successfully reached or exceeded them for 5 consecutive cycles. Fig. 4.7 shows an example of such adjustments, in which the target value was increased 4 times for  $T_{min}$  and 3 times for  $S_{max}$ . During the feedback conditions, all subjects except one (11 out of 12) were able to increase their  $T_{min}$  target at least twice, and all subjects except one (11 out of 12) increased their

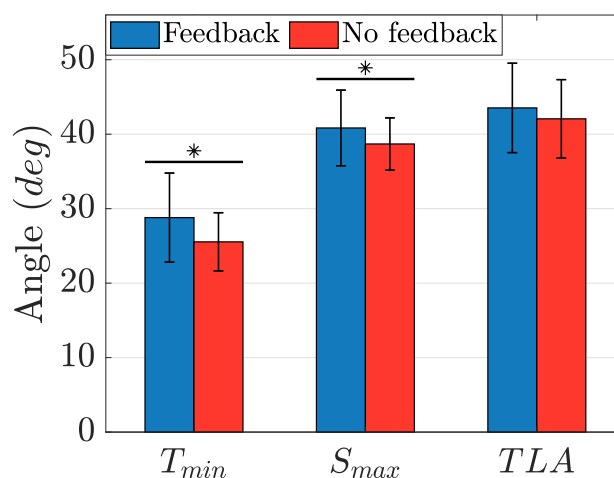


Figure 4.6: Comparison of the surrogates and  $TLA$  of the feedback and no-feedback sides in  $TS$  condition. Asterisks denote  $p < 0.05$ .

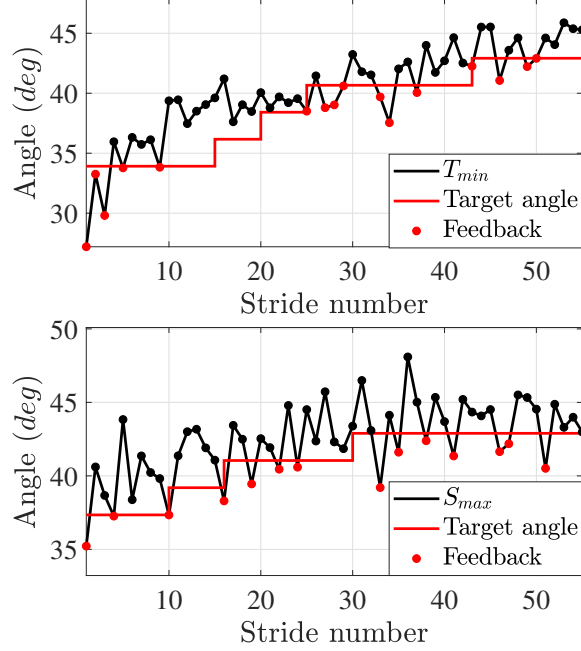


Figure 4.7:  $T_{min}$  (top) and  $S_{max}$  (bottom) compared to their targets. Gait cycles where haptic feedback was given to the segment are marked with red dots.

$S_{max}$  target angle at least twice. The two subjects that failed to achieve two increases were still able to do so once for the associated segment.

#### 4.2.5 Subjective Ratings by the Participants

The mean and standard deviation of subjects' rating to the questions were as follows: (a) level of comfort (thigh:  $8.17 \pm 2.95$ , shank:  $8.25 \pm 2.49$ ), (b) noticeability (thigh:  $8.33 \pm 1.56$ , shank:  $8.83 \pm 1.59$ ), (c) intuitiveness for reaching the target (thigh:  $7.25 \pm 2$ , shank:  $7.92 \pm 1.78$ ). Using Wilcoxon Signed-Rank test, we found no statistically significant difference between the ratings of the thigh and shank feedback methods for each question.

### 4.3 Discussion

#### 4.3.1 Spatiotemporal Parameters

When comparing the feedback conditions to normal and fast walking, the subjects were able to significantly increase their stride length. Gait speed was also at least 15% greater than normal walking. Fig. 4.4 shows that the increase in speed during self-selected fast

walking was due to larger values of both stride length and cadence. However, in the feedback conditions, the increase in speed was mainly due to the increase in stride length. As mentioned earlier, previous studies have found that walking speed decline in older adults is caused by a decrease in stride length; thus, our results show promise for enhancing stride length and, thereby, gait speed in that population.

### 4.3.2 The Biomechanical Surrogates and TLA

The results indicated that (1) the surrogates significantly increased by the haptic feedback, and (2) those increases were translated into higher values of stride length and speed. In our initial statistical analysis, we found that increasing  $T_{min}$  and  $S_{max}$  was positively correlated with stride length (i.e., correlation effect). Given the results of our experiment (Fig. 4.5), the changes in those variables via haptic feedback resulted in increased stride length and speed indicating a causation effect and supporting our hypothesis of choosing them as the biomechanical surrogates for stride length.

The subjects conveniently exceeded the initial target values of both the thigh and shank, demonstrating the efficacy of the haptic system in modifying the surrogates. Interestingly, the absence of significant difference in  $S_{max}$  among the feedback conditions indicates that providing feedback to the thighs alone could modify the gait such that the increase of  $S_{max}$  is also attained. In Chapter 2, we chose  $S_{max}$  as the second surrogate over  $F_{max}$  hypothesizing that increasing  $S_{max}$  would also increase  $F_{max}$ . The results demonstrated an increase of about 21% in  $F_{max}$  in the feedback conditions, supporting our hypothesis. We also found a consistent increase of  $TLA$  due to the application of haptic feedback. It is plausible that increasing  $T_{min}$  also increased the thigh angle close to toe-off which significantly contributes to  $TLA$  as previously reported [44]. Additionally, it is possible that the momentum necessary for increasing  $S_{max}$  at the end of the swing phase required a higher propulsive force in push-off and, thus, increased  $TLA$ . Overall, the

results imply that a higher propulsive force due to increased  $TLA$  by the haptic feedback was an underlying kinetic factor for increasing stride length and velocity.

### 4.3.3 Symmetry Between the Two Sides in the TS Trial

Further evidence for the efficacy of the haptic feedback is provided by the fact that the subjects increased  $T_{min}$  and  $S_{max}$  of the feedback side more than the other side in  $TS$  condition, and this condition was the only one with significant differences between the two sides. The lack of significant differences in the spatiotemporal parameters indicates that, although  $T_{min}$  and  $S_{max}$  increased more on the feedback side, this did not result in any significant gait asymmetry. It is possible that these between-side differences were not large enough to affect the high-level gait parameters or that the symmetry of spatiotemporal parameters was achieved by maintaining a similar value for other parameters such as  $TLA$  on both sides.

### 4.3.4 Adjustment to Haptic Feedback

Overall, 10 out of 12 subjects were able to not only reach the initial target values for both surrogates (i.e., with a larger than 54% of increase for  $T_{min}$  and more than 17% for  $S_{max}$ ), but also they increased the target values at least twice, which suggests that the selected initial targets were generally within the biomechanical limits of the subjects. The two subjects were still able to increase the target values once and reach the new targets; however, they could not maintain the changes for five consecutive cycles. This finding may have implications for personalizing training, where the initial target values can be automatically determined based on each individual's performance. One interesting observation from Fig. 4.7 is that the subject promptly responded to the applied feedback by trying to increase the intended surrogate and reach the new target values. Also, the fact that the subjects could adapt to new target values and gradually increase their surrogates further supports the system's efficacy in guiding the subject.

#### **4.3.5 Subjective Ratings by the Participants**

The subjects rated the tactile feedback for the thigh and shank similarly. In terms of perception, subject scores indicate that they found the feedback to be comfortable and noticeable during different walking conditions. The ratings for the intuitiveness suggest the tactile feedback and vibration duration could successfully inform the subjects about “how” to modify the intended variables. It is important to note that the subjects only used the system for 30 minutes in total; a longer training can further improve users’ performance and, consequently, enhance the system’s intuitiveness and efficacy.

## CHAPTER 5

### CONCLUSION

We developed a novel wireless, lightweight, and smartphone-based haptic system suitable for home- and community-based applications. A biomechanics-driven framework was established to provide tactile feedback for improving users' underlying gait variables (i.e., the surrogates) and, thereby, generate desired gait outcomes. The target values were chosen to encourage increasing the surrogates and investigate if and how such increases would translate into improved stride length and gait speed, and to obtain the range of increase in the surrogates during our training session. We showed the efficacy of our system in achieving that objective via conducting subject experiments and quantifying various gait parameters and subjective ratings of the participants. While this study recruited young participants to validate the proposed system and approach, future studies will focus on evaluating the presented biomechanics-driven surrogate approach and the haptic feedback for gait training of the target population of older adults. Other key parameters quantifying the users' overall gait will be considered to find the target values using more individualized methods such as human-in-the-loop optimization. Also, we will explore the effects of shorter and longer feedback durations on the users' gait parameters.

## REFERENCES

- [1] Mohsen Alizadeh Noghani, Mohsen Shahinpoor, and Babak Hejrati. “Design and Validation of a Smartphone-based Haptic Feedback System for Gait Training”. In: *IEEE Robotics and Automation Letters* 6.4 (2021), pp. 6593–6600.
- [2] Joe Verghese et al. “Epidemiology of Gait Disorders in Community-residing Older Adults”. In: *Journal of the American Geriatrics Society* 54.2 (2006), pp. 255–261.
- [3] Joe Verghese et al. “Abnormality of Gait as a Predictor of Non-Alzheimer’s Dementia”. In: *New England Journal of Medicine* 347.22 (2002), pp. 1761–1768.
- [4] Michelle M Mielke et al. “Assessing the Temporal Relationship Between Cognition and Gait: Slow Gait Predicts Cognitive Decline in the Mayo Clinic Study of Aging”. In: *Journals of Gerontology Series A: Biomedical Sciences and Medical Sciences* 68.8 (2013), pp. 929–937.
- [5] Neelum T Aggarwal et al. “Motor Dysfunction in Mild Cognitive Impairment and the Risk of Incident Alzheimer Disease”. In: *Archives of Neurology* 63.12 (2006), pp. 1763–1769.
- [6] Stacy Fritz and Michelle Lusardi. “White paper:“Walking Speed: the Sixth Vital Sign””. In: *Journal of Geriatric Physical Therapy* 32.2 (2009), pp. 2–5.
- [7] Pete B Shull et al. “Quantified Self and Human movement: a Review on the Clinical Impact of Wearable Sensing and Feedback for Gait Analysis and Intervention”. In: *Gait & Posture* 40.1 (2014), pp. 11–19.
- [8] Daniel K White et al. “Trajectories of Gait Speed Predict Mortality in Well-functioning Older Adults: the Health, Aging and Body Composition Study”. In: *Journals of Gerontology Series A: Biomedical Sciences and Medical Sciences* 68.4 (2013), pp. 456–464.
- [9] Susan E Hardy et al. “Improvement in Usual Gait Speed Predicts Better Survival in Older Adults”. In: *Journal of the American Geriatrics Society* 55.11 (2007), pp. 1727–1734.
- [10] Julien Dumurgier et al. “Slow Walking Speed and Cardiovascular Death in Well Functioning Older Adults: Prospective Cohort Study”. In: *BMJ* 339 (2009).
- [11] Joe Verghese et al. “Quantitative Gait Markers and Incident Fall Risk in Older Adults”. In: *The Journals of Gerontology: Series A* 64.8 (2009), pp. 896–901.
- [12] Monique M Samson et al. “Differences in Gait Parameters at a Preferred Walking Speed in Healthy Subjects due to Age, Height and Body Weight”. In: *Aging Clinical and Experimental Research* 13.1 (2001), pp. 16–21.
- [13] David A Winter et al. “Biomechanical Walking Pattern Changes in the Fit and Healthy Elderly”. In: *Physical Therapy* 70.6 (1990), pp. 340–347.
- [14] RJ Elble et al. “Stride-dependent Changes in Gait of Older People”. In: *Journal of Neurology* 238.1 (1991), pp. 1–5.

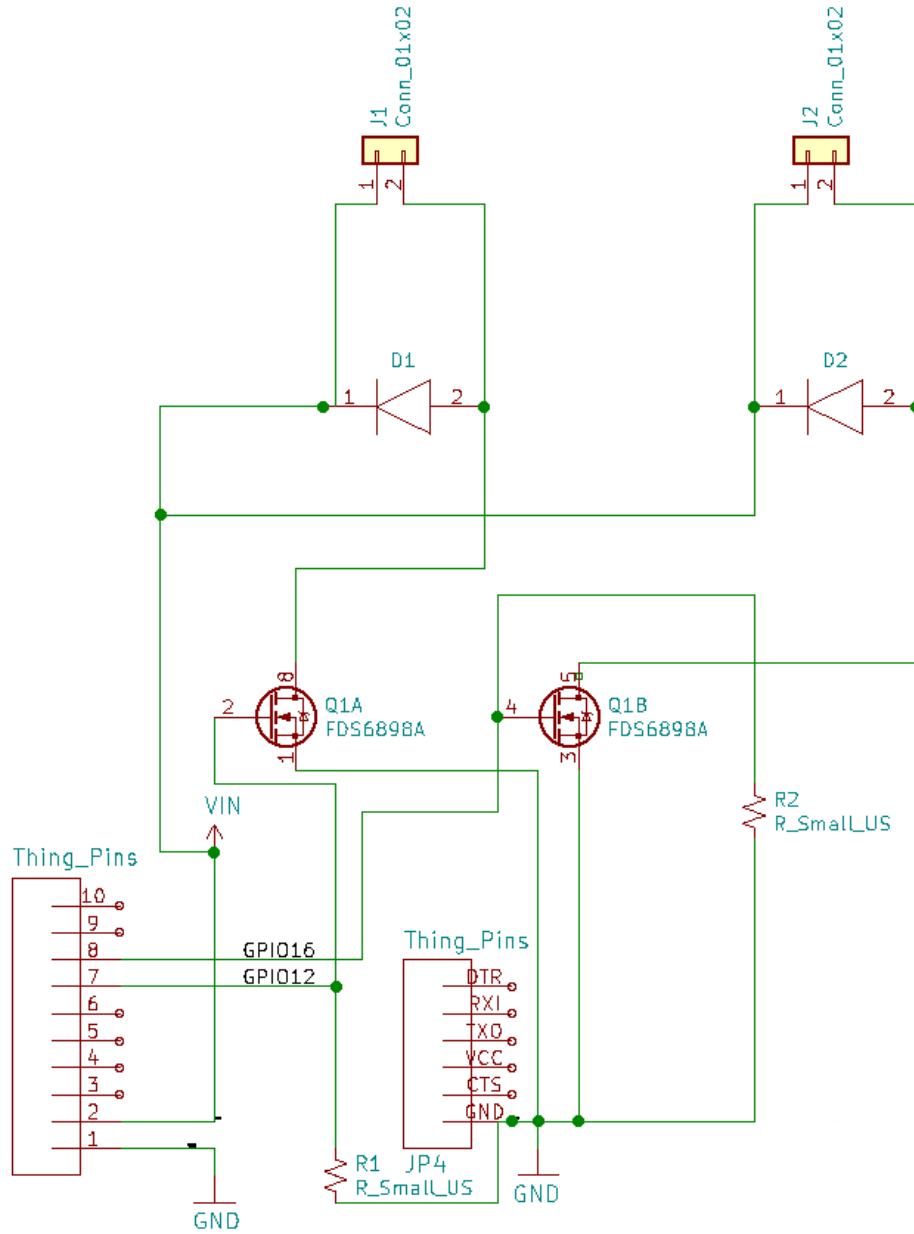
- [15] Hylton B Menz et al. “Reliability of the GAITRite® Walkway System for the Quantification of Temporo-spatial Parameters of Gait in Young and Older people”. In: *Gait & Posture* 20.1 (2004), pp. 20–25.
- [16] Bernard Auvinet et al. “Reference Data for Normal Subjects Obtained with an Accelerometric Device”. In: *Gait & Posture* 16.2 (2002), pp. 124–134.
- [17] Karen M Ostrosky et al. “A Comparison of Gait Characteristics in Young and Old Subjects”. In: *Physical Therapy* 74.7 (1994), pp. 637–644.
- [18] Roland Sigrist et al. “Augmented Visual, Auditory, Haptic, and Multimodal Feedback in Motor Learning: A Review”. In: *Psychonomic Bulletin & Review* 20.1 (2013), pp. 21–53.
- [19] Antonio Rodriguez-Fernández, Joan Lobo-Prat, and Josep M Font-Llagunes. “Systematic Review on Wearable Lower-limb Exoskeletons for Gait Training in Neuromuscular Impairments”. In: *Journal of Neuroengineering and Rehabilitation* 18.1 (2021), pp. 1–21.
- [20] Jennifer S Brach and Jessie M VanSwearingen. “Interventions to Improve Walking in Older Adults”. In: *Current Translational Geriatrics and Experimental Gerontology Reports* 2.4 (2013), pp. 230–238.
- [21] Jason W Wheeler, Pete B Shull, and Thor F Besier. “Real-time Knee Adduction Moment Feedback for Gait Retraining Through Visual and Tactile Displays”. In: *Journal of Biomechanical Engineering* 133.4 (2011).
- [22] Christopher Schenck, Duncan Bakke, and Thor Besier. “Haptic Biofeedback Induces Changes in Ankle Push-off During Walking”. In: *Gait & Posture* 74 (2019), pp. 76–82.
- [23] Kelly R Sheerin et al. “The Effectiveness of Real-time Haptic Feedback Gait Retraining for Reducing Resultant Tibial Acceleration with Runners”. In: *Physical Therapy in Sport* 43 (2020), pp. 173–180.
- [24] Thiago Braga Rodrigues et al. “A Quality of Experience Assessment of Haptic and Augmented Reality Feedback Modalities in a Gait Analysis System”. In: *Plos One* 15.3 (2020), e0230570.
- [25] Ariel V Dowling, David S Fisher, and Thomas P Andriacchi. “Gait Modification via Verbal Instruction and an Active Feedback System to Reduce Peak Knee Adduction Moment”. In: (2010).
- [26] Pete B Shull et al. “Training Multi-parameter Gaits to Reduce the Knee Adduction Moment with Data-driven Models and Haptic Feedback”. In: *Journal of Biomechanics* 44.8 (2011), pp. 1605–1609.
- [27] Daniel KY Chen, Markus Haller, and Thor F Besier. “Wearable Lower Limb Haptic Feedback Device for Retraining Foot Progression Angle and Step Width”. In: *Gait & Posture* 55 (2017), pp. 177–183.
- [28] Junkai Xu et al. “Configurable, Wearable Sensing and Vibrotactile Feedback System for Real-time Postural Balance and Gait Training: Proof-of-concept”. In: *Journal of Neuroengineering and Rehabilitation* 14.1 (2017), pp. 1–10.

- [29] Haisheng Xia et al. “Portable, Automated Foot Progression Angle Gait Modification via a Proof-of-concept Haptic Feedback-sensorized Shoe”. In: *Journal of Biomechanics* 107 (2020), p. 109789.
- [30] Huanghe Zhang et al. “Wearable Biofeedback System to Induce Desired Walking Speed in Overground Gait Training”. In: *Sensors* 20.14 (2020), p. 4002.
- [31] Pete B Shull et al. “Toe-in Gait reduces the First Peak Knee Adduction Moment in Patients with Medial Compartment Knee Osteoarthritis”. In: *Journal of Biomechanics* 46.1 (2013), pp. 122–128.
- [32] Pete B Shull et al. “Six-week Gait Retraining Program Reduces Knee Adduction Moment, Reduces Pain, and Improves Function for Individuals with Medial Compartment Knee Osteoarthritis”. In: *Journal of Orthopaedic Research* 31.7 (2013), pp. 1020–1025.
- [33] Babak Hejrati et al. “Comprehensive Quantitative Investigation of Arm Swing During Walking at Various Speed and Surface Slope Conditions”. In: *Human Movement Science* 49 (2016), pp. 104–115.
- [34] Roger W Cholewiak and James C Craig. “Vibrotactile Pattern Recognition and Discrimination at Several Body Sites”. In: *Perception & Psychophysics* 35.6 (1984), pp. 503–514.
- [35] Emel Demircan et al. “Perception Accuracy of Vibrotactile Feedback During Locomotion”. In: *2019 16th International Conference on Ubiquitous Robots (UR)*. IEEE. 2019, pp. 673–677.
- [36] EC Wentink et al. “Vibrotactile Stimulation of the Upper Leg: Effects of Location, Stimulation Method and Habituation”. In: *2011 Annual International Conference of the IEEE Engineering in Medicine and Biology Society*. IEEE. 2011, pp. 1668–1671.
- [37] Myrthe A Plaisier, Lotte IN Sap, and Astrid ML Kappers. “Perception of Vibrotactile Distance on the Back”. In: *Scientific Reports* 10.1 (2020), pp. 1–7.
- [38] Hesham Elsayed et al. “VibroMap: Understanding the Spacing of Vibrotactile Actuators across the Body”. In: *Proceedings of the ACM on Interactive, Mobile, Wearable and Ubiquitous Technologies* 4.4 (2020), pp. 1–16.
- [39] Ronald T Verrillo. “Age Related Changes in the Sensitivity to Vibration”. In: *Journal of Gerontology* 35.2 (1980), pp. 185–193.
- [40] Bruno Siciliano, Oussama Khatib, and Torsten Kröger. *Springer Handbook of Robotics*. Vol. 200. Springer, 2008.
- [41] Kristen L Lurie et al. “Informing Haptic Feedback Design for Gait Retraining”. In: *2011 IEEE World Haptics Conference*. IEEE. 2011, pp. 19–24.
- [42] Andria Farrens, Maria Lilley, and Fabrizio Sergi. “Training Propulsion via Acceleration of the Trailing Limb”. In: *IEEE Transactions on Neural Systems and Rehabilitation Engineering* (2020).
- [43] Angelo M Sabatini et al. “Assessment of Walking Features from Foot Inertial Sensing”. In: *IEEE Transactions on Biomedical Engineering* 52.3 (2005), pp. 486–494.

- [44] Takasuke Miyazaki et al. “Validity of Measurement for Trailing Limb Angle and Propulsion Force During Gait using a Magnetic Inertial Measurement Unit”. In: *BioMed research international* 2019 (2019).
- [45] Babak Hejrati et al. “Kinesthetic Force Feedback and Belt Control for the Treadport Locomotion Interface”. In: *IEEE Transactions on Haptics* 8.2 (2015), pp. 176–187.

## APPENDIX A

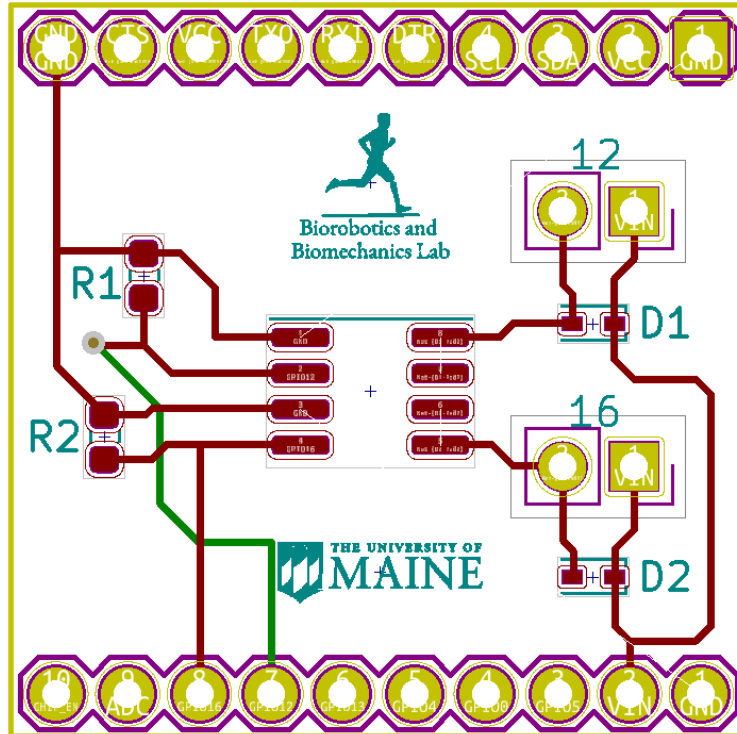
### SCHEMATIC OF THE MOTOR DRIVER PCB



| Part     | Digi-Key number  | Part description                |
|----------|------------------|---------------------------------|
| MOSFET   | FDS6898ACT-ND    | MOSFET 2N-CH 20V 9.4A 8SOIC     |
| Diode    | BAT54HT1GOSCT-ND | DIODE SCHOTTKY 30V 200MA SOD323 |
| Resistor | 311-1.0KGRCT-ND  | RES SMD 1K OHM 5% 1/1-W 0603    |

Table A.1: The electronic parts used for the motor driver PCB.

APPENDIX B  
LAYOUT OF THE MOTOR DRIVER PCB



## APPENDIX C

### THE PILOT PERCEPTION STUDY

We performed experiments with 4 older-adult participants to determine whether they could accurately perceive tactile signals in the form of vibrations on their thighs, and explored the feedback’s parameters in terms of the application location and the pulsation frequency (i.e. the number of on-off cycles of the tactile signal) that would result in the highest perceptibility.

The main components of the system and the process of the experiment are shown in Fig. C.1. The haptic cells were initially placed in custom-made pockets on four sides—anterior, lateral, posterior, and medial—of the shorts worn by the subjects. However, the medial location was found to be unsuitable mainly due to the short distance between the thighs causing repeated contacts between the cells and, therefore, damaging the motors’ connections. As the figure shows, the haptic cells were connected to a Raspberry Pi 4 (RPi 4) via a custom PCB which was mounted on RPi 4 and supplied the power and the driving signal to the haptic cells. The entire system, consisting of the RPi 4, the PCB, and the battery powering them was placed into a waist bag worn by the subject. Therefore, the system was completely portable, allowing the subject to walk without constraint. To avoid biasing the results, the order of the three trials also varied from subject to subject.

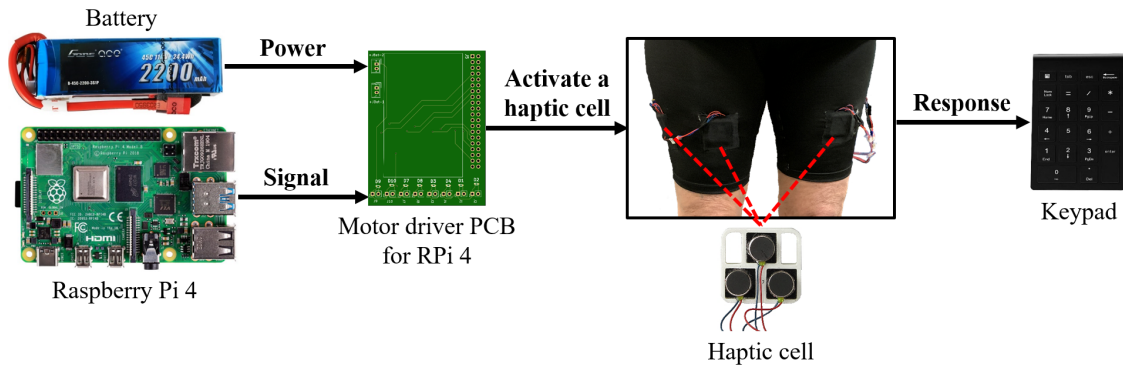


Figure C.1: Schematic of the system designed for the pilot perception experiment.

The subjects received tactile feedback in three trials: (1) while standing (static), and walking at their self-selected (2) normal and (3) fast speeds. During each experimental trial, vibration cues were given from all the six cells on the subjects' thighs in a random order. To minimize the possibility that the subject used auditory cues to locate the stimulus, they wore a wireless headphone (Fig. C.2a) which played white noise. Additionally, after the subject entered a response, a chime was played to indicate whether it was recorded successfully.

Four cases of 0, 2, 5, and 10 pulses were tested, in which the total duration of each vibration was chosen to be 0.5 sec. Zero (0) pulses meant a continuous vibration with the duration of 0.5 sec, whereas 2 pulses meant that the motor would turn on and off twice during the 0.5 sec interval. To detect false positives and false negatives, a "No vibration" condition was added where no cell was activated and the subject would have to respond by pressing the corresponding key on the keypad (Fig. C.2b). During the trials, each cell vibrated with all the possible combinations of location and number of pulses. Each combination was repeated six times resulting in twenty-four total vibrations at each location. The "No vibration" condition was also repeated twenty-four time in each trial. The subjects' responses were collected via the wireless keypad and recorded on the RPi 4. The accuracy of response was defined as the number of correct identification of a location over the total number of tactile feedback at that location (i.e., 24). The percentage accuracy of identifying the feedback location was used as the measure of perceptibility, and it was obtained for each location for all the applied pulsing conditions, and similarly for each pulsing condition for all locations.

The minimum accuracy score required for a location to be considered sufficiently perceptible was calculated based on a binomial distribution. Each response was assumed to be either true or false with the probability of 50% and therefore was considered as an outcome of a binomial distribution. As a criteria for specifying a threshold for an acceptable accuracy, we calculated the smallest number of correct answers (i.e., successes)

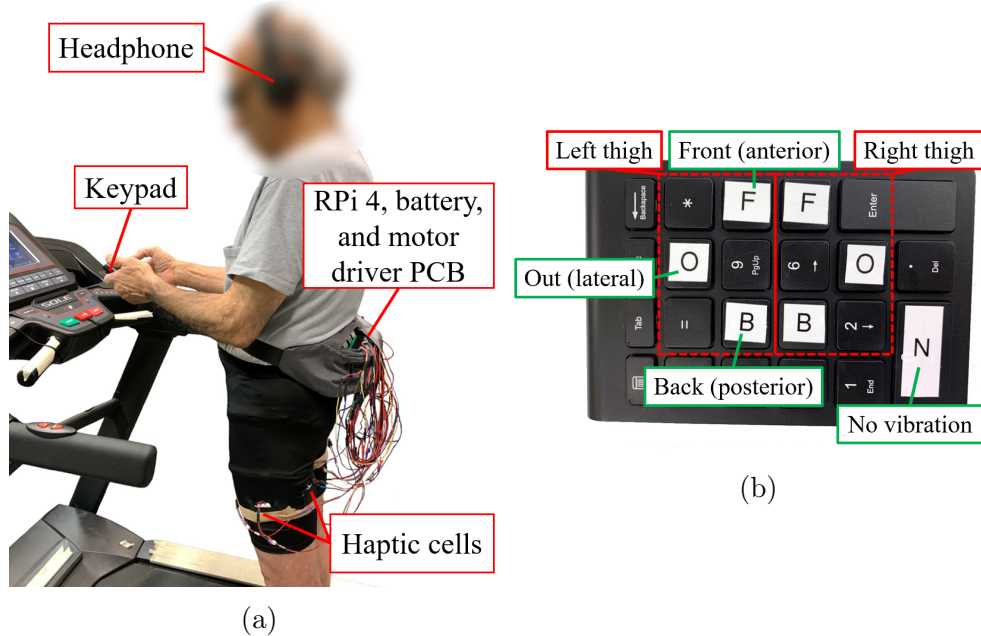


Figure C.2: (a) A subject using the system during the static (i.e. standing) trial on a treadmill. (b) The labeled keypad used by the subjects to submit their responses.

with less than 1% probability that they had been selected purely by chance [45]. For the binomial random variable measuring the number of successes by  $X$  and the probability of success by  $p$ , the probability for  $x$  successes is given by Equation C.1:

$$P(X = x) = 1 - B(x; n, p) \rightarrow P(X = 18) = 0.00331 \quad (\text{C.1})$$

where  $B(x, n, p)$  is the cumulative density function of the binomial distribution. As mentioned above, for our experiment, we assumed that the probability of a correct answer is  $p = 1/2$ , which is a conservative assumption given there were three choices for the location making the success probability  $p = 1/3$ . For the total trial  $n = 24$  for each location, the smallest  $x$  for which  $P(X = x)$  is smaller than 0.01 was found to 18, which corresponds to an accuracy of 75%.

Five subjects (4 males, 1 female,  $67.4 \pm 5.4$  years,  $1.77 \pm 0.07$  m,  $77.7 \pm 10.5$  kg) participated in the experiment. Figure C.3 provides a summary of the perception experiment results by combining the accuracy numbers for both right and left legs at different location and for different number of pulses. It can be seen that the accuracy levels

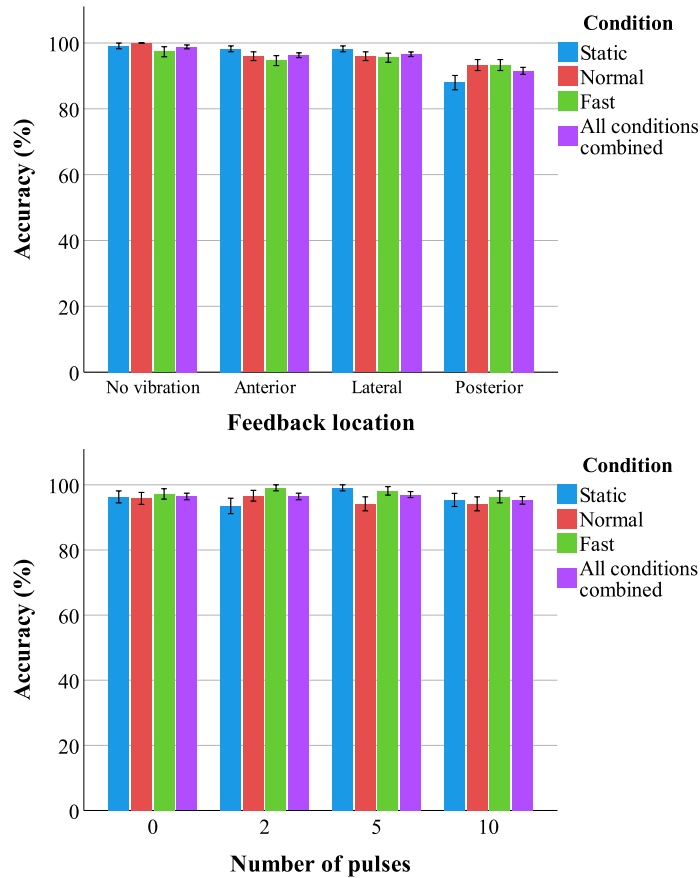
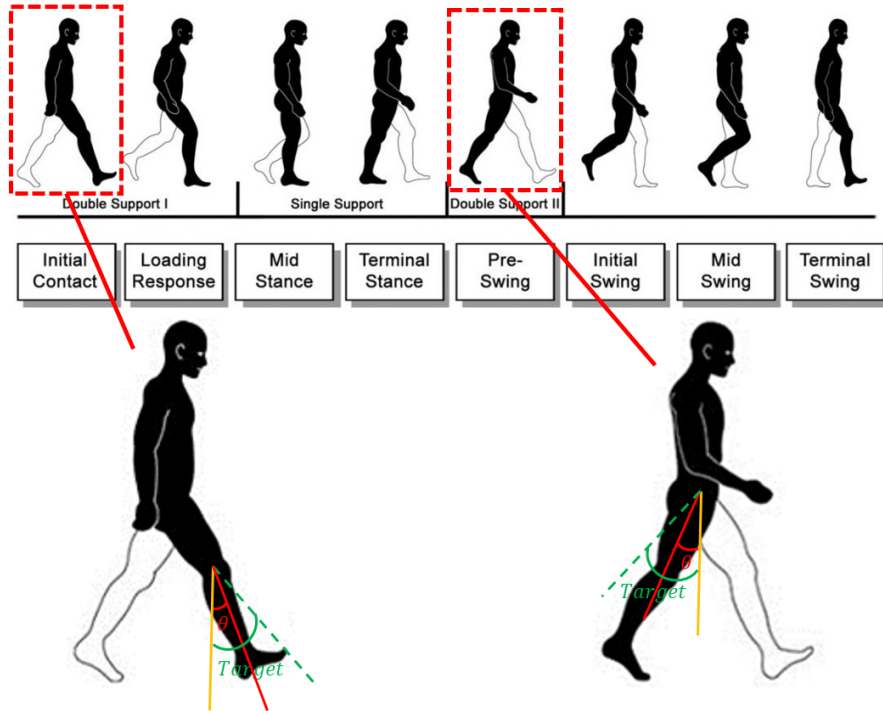


Figure C.3: Response accuracy at different locations (top) and for different number of pulses (bottom). 0 pulses means continuous vibration for 0.5 sec. Error bars represent  $\pm 1$  standard error.

for all the conditions and locations were above the required 75% threshold. The false negative rate (subjects perceiving no vibration when in fact a cell had been activated) was 0.256% and the false positive rate (subjects perceiving a vibration from a cell when there was none) was 1.73%, the majority (67%) of which was associated with falsely perceiving a vibration in the posterior cells. Further, because 0 pulses (i.e., 0.5 sec of continuous vibration) was associated with a high accuracy across all trials, it was selected as feedback scheme. Overall, the results indicate that not only were the subjects able to perceive the tactile feedback, but also they could accurately identify the location of feedback across all walking conditions.

## APPENDIX D

### INSTRUCTION SHEET SHOWN TO THE SUBJECTS



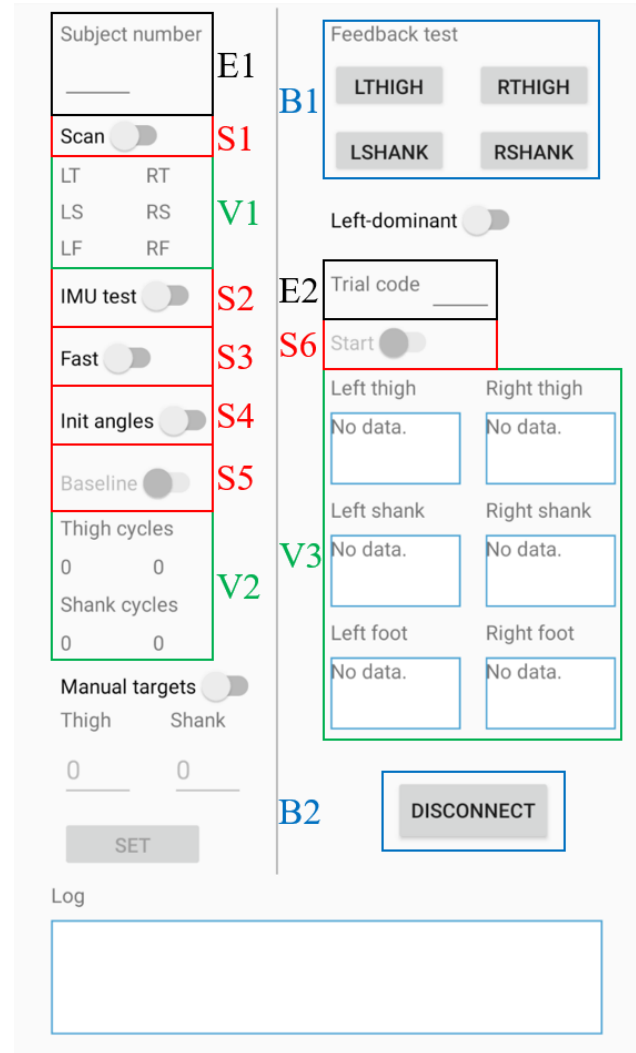
$\theta < Target$ : You receive feedback. Try to increase  $\theta$  next time.

$\theta \geq Target$ : You don't receive feedback. Try to maintain your current gait.

## APPENDIX E

### PROCEDURE FOR OPERATING THE ANDROID APPLICATION

- (1) Enter a number for the subject in E1.
- (2) Enable S1 to scan for sensors.
- (3) Wait until the text for each sensor in V1 is replaced with R, which means the sensor is ready to start measurement. At that point, you may disable S1.
- (4) Enable S2 to ensure that data is being received properly from the sensors. The textviews in V3 will be updated at 60 Hz.
- (5) Click on the buttons in B1 to ensure that the vibrotactors turn on for 0.5 second.
- (6) Enable S3 to start measurement for the fast walking ( $F$ ) trial. Disable to stop the measurement when the trial is done.
- (7) Enable S4 to initialize the sagittal angles (i.e., calculate  $\theta_0$ ).
- (8) Enable S5 to start the normal walking trial ( $N$ ). The cycles counted using the peak detection algorithm will be displayed in V2. After the initial cycles are obtained, the calculated values of the initial target will be displayed in V2 for each segment. Disable S5 to stop measurement.
- (9) Enter the code for a feedback trial in E2. For example, the codes for thigh familiarization is 1 and  $TT$  are 1 and 2, respectively.



(10) Enable S4 to initialize the angles. This should be done before starting each feedback trial.

(11) Enable S6 to start the feedback trial.

(12) By clicking B2, the sensors will be disconnected. To reconnect, you have to enable S1.

## **BIOGRAPHY OF THE AUTHOR**

Mohsen Alizadeh Noghani was born in Mashhad, Iran and graduated from Shahid Hashemi Nejad 1 high school in the same city. He earned his B.Sc. in Mechanical Engineering from Ferdowsi University of Mashhad in 2018. He is a candidate for the Master of Science degree in Mechanical Engineering from the University of Maine in August 2021.